CAPITAL UNIVERSITY OF SCIENCE AND TECHNOLOGY, ISLAMABAD

MINIATURIZED HIGH POWER RF SPDT SWITCH FOR UAV INTERROGATOR SYSTEM

by

Muhammad Kashif Latif

A thesis submitted in partial fulfillment for the degree of Master of Science

in the

Faculty of Engineering
Department of Electrical Engineering

2018

This work is dedicated to my parents, wife, children and Dr. Ali Imran for guiding me with love and patience.

CAPITAL UNIVERSITY OF SCIENCE & TECHNOLOGY
ISLAMABAD

CERTIFICATE OF APPROVAL

MINIATURIZED HIGH POWER RF SPDT SWITCH FOR UAV INTERROGATOR SYSTEM

by

Muhammad Kashif Latif
MEE151012

THESIS EXAMINING COMMITTEE

S. No.	Examiner	Name	Organization
(a)	External Examiner	Dr. Junaid Mughal	CIIT, Islamabad
(b)	Internal Examiner	Dr. Noor Muhammad Khan	CUST, Islamabad
(c)	Supervisor	Dr. Ali Imran Najam	CUST, Islamabad

Supervisor Name
Dr. Ali Imran Najam
May 2018

Dr. Noor Muhammad Khan
Head
Dept. of Electrical Engineering
May 2018

Dr. Imtiaz Ahmed Taj
Dean
Faculty of Engineering
May 2018

Author's Declaration

It is declared that this is an original piece of my own work, except where otherwise acknowledged in text and references. This work has not been submitted in any form for another degree or diploma at any university or other institution for tertiary education and shall not be submitted by me in future for obtaining any degree from this or any other University or Institution.

(Muhammad Kashif Latif)

Registration No: MEE151012

Plagiarism Undertaking

I solemnly declare that research work presented in this thesis titled "*Miniaturized High Power RF SPDT switching design for UAV Interrogator System*" is solely my research work with no significant contribution from any other person. Small contribution/help wherever taken has been dully acknowledged and that complete thesis has been written by me.

I understand the zero tolerance policy of the HEC and Capital University of Science and Technology towards plagiarism. Therefore, I as an author of the above titled thesis declare that no portion of my thesis has been plagiarized and any material used as reference is properly referred/cited.

I undertake that if I am found guilty of any formal plagiarism in the above titled thesis even after award of MS Degree, the University reserves the right to withdraw/revoke my MS degree and that HEC and the University have the right to publish my name on the HEC/University website on which names of students are placed who submitted plagiarized work.

(Muhammad Kashif Latif)

Registration No: MEE151012

Acknowledgements

I am thankful to ALMIGHTY ALLAH, for giving me the strength and encouragement to accomplish the assigned tasks in the most appropriate manner including the research work presented in this thesis.

My Supervisor Dr. Ali Imran Najam is my mentor and I found him always standing by me to help me during my entire graduate program. Due to his sincere guidance and technical acumen, I am able to carry out the most difficult tasks with ease. It has been an honor to work under under his supervision. I am grateful to him from the core of my heart for his perseverance, management, illustrious advices, expedient suggestions, caring and vibrant supervision throughout my research work. His unorthodox approach towards solving difficult problems, valuable suggestions, constructive, co-operative and kind affectionate behavior resulted in completion of this thesis.

I am also thankful to the CUST administration for providing me an excellent platform for conduct of my MS thesis Studies research work.

I am also thankful to Dr. Mansoor Ahmed, Dr. Imtiaz Taj, Dr. Noor Muhammad, Dr. Amir Iqbal Bhatti, all teachers and staff members of CUST for their cooperation, help and valuable suggestions.

I am also using this opportunity to thank all my friends who prayed for me and encouraged me through their love and sincerity.

May ALLAH bless all these wonderful people

Abstract

In the modern era, unmanned aerial vehicles are gaining importance for its major contributions in scientific, commercial and military applications. The limited space on UAVs demands every aspect to be studied in detail for miniaturization. This thesis presents designing, simulation, fabrication and analysis of a miniaturized high power RF single port double throw switch for UAV interrogator radar system. The thesis covers a brief survery on available SPDT switches, techniques used in its design, parameters that affect the size and power handling capabilities of said switches. The standard toplogy of designing traditional RF SPDT switches is modified and the proposed design has been simulated using Advanced Design Software ADS 2016 on IFF interrogator frequency of 1030 MHZ. Aspects related to power handling along with miniaturization of substrates available are calculated and discussed for choosing the most suitable design. The circuitry is simulated using properties of Rogers RT/Duroid 6010.2LM substrate and desired simulated results of insertion loss less than 1 dB and isolation between the ports greater than 30 dB are achieved. Layout of SPDT switch has been designed in ADS 2016 for fabrication within a small size of 25x25 sq mm and the fabricated module has been tested in the real environmment. The performance of the designed SPDT switch is evaluated by comparing it with the measured results.

Contents

List of Figures

List of Tables

Abbreviations

PSR	Primary Surveillance Radar
SSR	Secondary Surveillance Radar
IFF	Identification Friends and Foe
RF	Radio Frequency
PRF	Pulse Repetition Frequency
T/R	Transmitter Receiver
DS	Diversity Selective
EM	Electro-mechanical
FET	Field Effect Transistors
RL	Return Loss
VSWR	Voltage Standing Wave Ratio
SPST	Single Pole Single Throw
SPDT	Single Pole Double Throw
ADS	Advanced Design system
VNA	Vector Network Analyzer
IL	Insertion Loss
DUT	Device Under Test

Symbols

τ	Carrier lifetime
P_D	Maximum average power dissipation
C_T	Total capacitance in reverse bias condition
R_p	Parallel resistance when PIN diode is reverse bias
R_s	Series resistance of a PIN diode when it is forward bias
V_r	Reverse breakdown voltage
ϵ	Dielectric constant
ϵ_r	Dielectric constant of medium
A	Area of diode junction
V^+	Incident voltage wave amplitude
V^-	Reflected voltage wave amplitude
Γ	Voltage reflection coefficient
Z_O	Characteristic impedance
Z_L	Load impedance
T_{FR}	Forward bias to reverse bias transition time
T_{RF}	Reverse bias to forward bias transition time
P_{av}	Maximum available power
V_g	Generator voltage
Z_{in}	Input impedance
$Z_{microstrip}$	Microstrip line impedance
w	Conductor width
h	Substrate thickness
t	Conductor thickness

Chapter 1

Introduction

1.1 Background

The research and development in this technological world is progressing at a fast pace with evolution of latest techniques implemented for improvements in all fields. The technological world has come far way ahead and big old machines are being converted into small machines capable of undertaking the tasks in a more proficient manner. The concept of miniaturization has evolved progressively in all fields of science and technology. In the field of computer science, the world has seen the first computer with a big size of 167 sq meters being converted into a chip sized less than half a centimeter size computer named as Michigan Micro Mote (M3) [1].

Similarly, the aviation industry is progressing rapidly and flying machines with

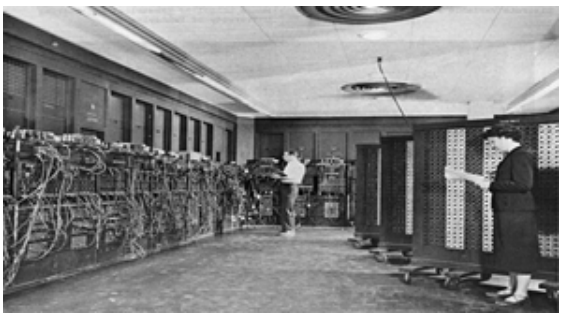

FIGURE 1.1: World First Computer [1]

miniaturized design is the need of hour for undertaking multi-dimensional tasks in

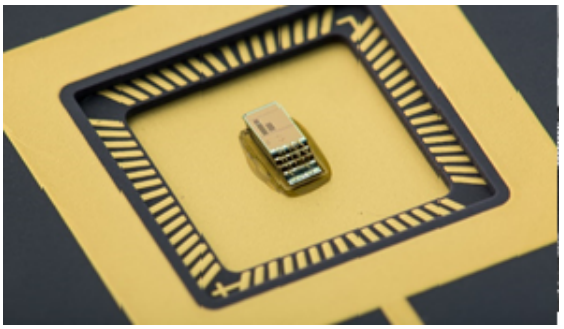

FIGURE 1.2: Michigan Micro Mote (M3) [1]

an effective way [2]. The drones and UAVs are being used in almost every field of human world including medical assistance at hard to reach places, surveillance of area through UAVs, attacking of enemy through drones with no danger of human loss, bomb detection, journalism, disaster management etc [3]. The scope of using

FIGURE 1.3: Multidimensional uses of drones [3]

these mini flying machines as radars is being studied worldwide, however, the limited space on these flying machines requires every aspect of radar to be studied in detail. Conversion of radars capable of handling high RF power is not only challenging due to limited space available on small UAVs but also requires a very sophisticated design for handling such high power. Since radar technology mainly depends upon the transmission power for the area coverage; generation of high transmission power along with its transmission are the major challenges being experienced. Therefore, the need to study and convert various modules of radars into a miniaturized size capable of handling high power is a continuous process and being studied world-wide [4]. The radar systems are broadly categorized into two portions i.e primary surveillance radar and secondary surveillance radar.

1.2 Primary Surveillance Radar

Primary surveillance radar (PSR) works on the principal of transmission of high power RF energy and subsequent detection of reflected energy from the airborne platforms within their range. The range of PSR mainly depends upon the power with which the RF signal is transmitted. Therefore, amplification of RF signals to a certain level determines the range of radar systems and thus, requires extreme care while designing the system. PSR is mostly used in case of military applications for detection of unknown aircraft [5]. The basic PSR principle is shown in Figure (1.4).

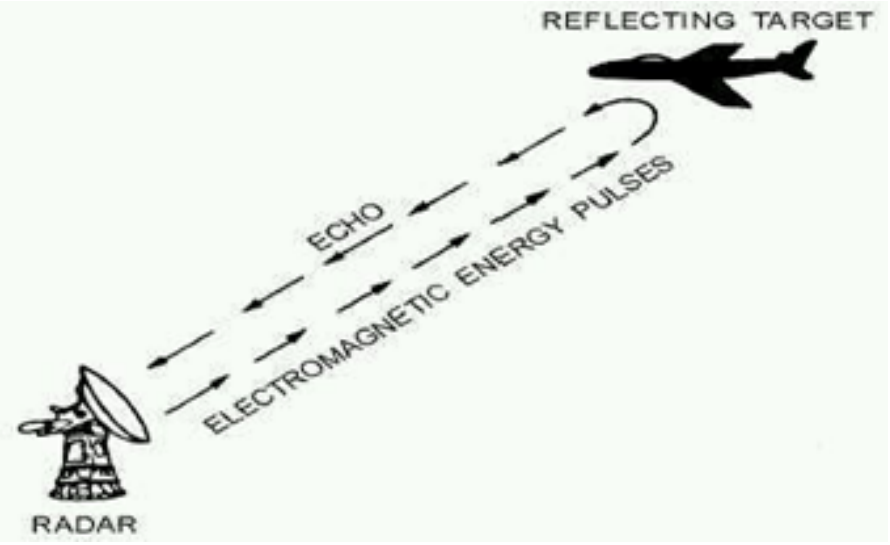

FIGURE 1.4: Primary Surveillance Radar Principle [5]

1.3 Secondary Surveillance Radar (SSR)

The second most important element in a radar is the secondary surveillance radar system primarily designed for air traffic command and control of aerial fields. It works on the principle of identification of friend or foe (IFF) and enables aircraft controllers to know the exact location of aircraft. An interrogation station transmits a coded interrogation RF modulated signal at 1030MHz. Transponders,

which are carried on the airplanes interrogated, are triggered by the coded interrogation signal to produce and transmit a response (or reply) signal on 1090MHz [6]. Figure (1.5) illustrates the operating principle of IFF.

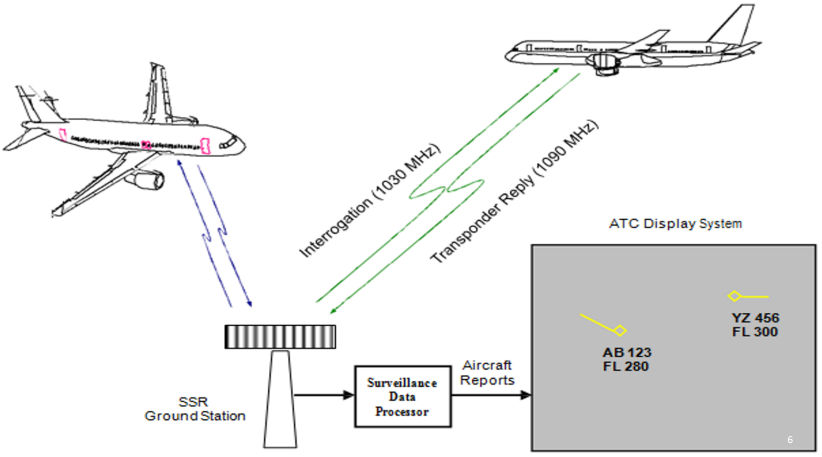

FIGURE 1.5: Working principle of IFF [6]

Secondary surveillance radar is designed to be operated like a transmitter and a receiver of radar system. SSR provides 360 degree coverage using directional antenna system [6]. The range is determined using the time lapse between the transmission and reception pulses and synchronized antenna rotation provided information of correct bearing of the aircraft.

1.4 Interrogation Modes

Interrogation modes are the key elements of an IFF system and provides information related to various parameters of aircraft depending upon the spacing between the transmitted pulses. These transmitted pulses are generally indicated as P1 & P3 and lays the foundation of IFF system mechanism. However, the side lobes are being generated for these pulses due to directional antenna system, thereby making the aircraft prone to unnecessary replies. Thus, unnecessary replies to various side lobe system pulses of different radar system would paint a completely different picture on the radar scope. To overcome this phenomenon, the radar systems are provided with a second mainly omni-directional antenna with its beam

having gain exceeding that of the sidelobes but not that of the main beam (Figure (1.6)). A third pulse, P2, is transmitted from this second beam 2 s after P1 [7]. An aircraft detecting P2 stronger than P1 (therefore in the sidelobe and at the incorrect main lobe bearing), does not reply.

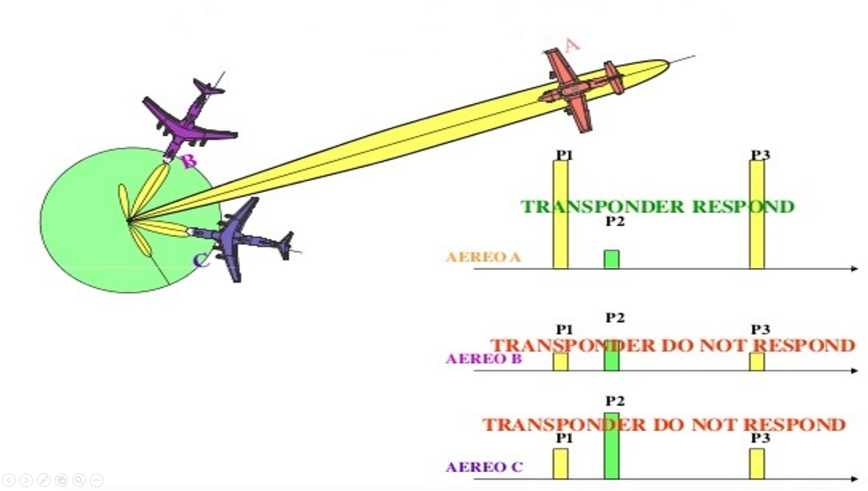

FIGURE 1.6: IFF Interrogator Pulses Response [7]

Since the IFF interrogators are being used in all SSR systems, the reliability of information of aircraft depends on the correct transmission of pulses.
In addition to performance constraints, the SPDT switch is required to be able to handle the high power being transmitted by the interrogator along with minimal size to counter for constraint space availability in the system. The main function of SPDT switch is to direct the high power transmission pulse either to Antenna 1 or Antenna 2 with low insertion loss and high isolation between dual antennas.

1.5 Problem Statement

The major consideration of the design is the **miniaturized** single port double throw RF switch that is required to handle an **output power of 60 dBm** taking into consideration the high isolation between transmission pulse channels. The challenge is to design a high isolation between the dual transmission pulse channels for two antenna systems to avoid interference, and overlapping, while maintaining

minimum insertion loss is also crucial so that accurate transmission of pulses can be made possible.

1.6 Objective

The objective of this research is to design, simulate, fabricate and analyze the single port double throw RF switch to achieve an isolation of greater than 30dB between the antenna systems and insertion loss of less than 1dB keeping in consideration the required output power of around 60 dBm within smallest possible size.

1.7 Summary

In this chapter, the research background, problem statement and objective is stated clearly so that the reader could have a clear understanding about this research.

Chapter 2

RF SWITCHING TECHNIQUES

2.1 Introduction

The concept of RF switch revolves around the directional communication of high frequency RF signals over a combined path between the ports and separate RF ports from each other. In this chapter a compact synopsis on the basic types and features of RF switches are discussed. The details related to the pin diode are discussed briefly along with reasons for its suitability in the RF switching mechanism. In this chapter it is discussed that pin diode is the best suitable device to be used in this applications requiring miniature size with good performance.

2.2 RF Switch

RF switches are the key elements in radar and radioi frequency communication systems being used in the world. RF switch has the capability to control the burst of RF energy in the circuit between particular ports and serves in maintaining isolation level between the devices at ports within an acceptable range. RF switches can further be divided into following categories:

- Electro Mechanical (EM)

- Field Effect Transistors (FET)
- PIN diodes
- Hybrid

2.2.1 Electro Mechanical RF Switches

The size of EM RF switches are substantially large as these are made up of coils and mechanical contacts. The major advantage of these switches is that they can function from lower (dc) up to higher frequencies (50+ GHz). Electrostatic discharge (ESD) effects on these switches are negligible and can be used in environments having higher risk of ESD affects. The operational issues of mechanical switches includes the limited operating life and increase in insertion loss due to change of resistance values in mechanical contacts. On the other hand, RF switches made by diodes and transistors commonly known as solid state RF switches has higher operating life and are resistant to vibrations and jolts [9].

2.2.2 Field Effect Transistor Based RF switches

Field Effect Transistor (FET) is made up of a semi-conductor material whose electric field manages the conductivity of a channel [9]. Gate, drain and source are the main terminals of FET. Gate voltages controls the current between source and drain terminals when voltage is applied between them. FET switches are stable due to good control of drain to source resistance, However, the major drawback of FET switches is that its isolation degrades as the frequency increases due to drain-to source capacitance (CDS) effect. The capacitance at high frequencies between drain terminal and source terminal deteriorates the isolation in the switch. The signal quality of the FET is capable enough to reduce insertion-loss in comparison with other switching technologies [9].

2.2.3 PIN diode RF switches

A PIN diode is a diode with a wide, un-doped intrinsic semiconductor region between a p-type semiconductor and an n-type semiconductor region. The p-type and n-type regions are typically heavily doped because they are used for ohmic contacts. It is controlled by changing its operating state between forward bias and reverse biased depending upon the biasing voltages applied at its terminals. It can be used as a switching device when control current is switched in discrete steps. High switching speed, fast settling time, excellent rise and fall time, small physical size, high power handling and low parasitic reactances make it an ideal choice for use in RF high power switching applications [10].

2.2.4 Hybrid RF Switches

Combination of PIN diode and FET are used to make hybrid switches. FETs are used in said switches to increase the frequency response upto DC having acceptable isolation and shunt PIN diodes are used at $\lambda/4$ spacing in order to have good isolation at various high frequencies. Main disadvantage of using these types of switches is they usually have bigger size and offer higher insertion loss [10].

2.2.5 Comparison

Figure 2.1 shows the general comparison of RF Switches [11]. It has been observed that PIN diodes provides fast switching speed, better insertion loss and high power handling in comparison with FET RF switches or Hybrid RF switches. Its use in SPDT switch for controlling RF signal offers tremendous rise and settling time performance, better insertion loss and isolation in comparison to FET or hybrid switches. Therefore, PIN diode is preferable to be used in SPDT switch and will further be elaborated in coming paragraphs.

Switch Type	Electro-Mechanical	Solid State		
		FET	PIN	Hybrid
Frequency Range	DC ~ 20 GHz		10 MHz to 50 GHz	300 kHz to 20 GHz
Insertion Loss	Average (greater than 1dB)	**Good** (less than 1dB)	**Good** (less than 1dB)	Average (greater than 1dB)
Isolation	Good (Greater than 50 dB)	Good at low frequencies (Greater than 80 dB)	Good at high Frequency only (Greather than 50 dB)	
Switching Speed	Milliseconds	Microseconds	Nano seconds	Microseconds
Rise / fall time	Milliseconds	Microseconds	Nanoseconds	Microseconds
Switching on/off	Milliseconds	Microseconds	Nanoseconds	Microseconds
Power Handling	High	Low	High	Low
Operating Life	Limited depends upon usage	Long life due to Solid State Technology		
Suspceptible to	Vibrations	Temperature and RF power extremes		

FIGURE 2.1: RF switch comparison [11]

2.3 Characteristics of PIN Diode Based Switching

At lower frequencies, PIN diode behaves as a normal diode and follows standard diode equation. However, at higher frequencies, the diode behaves as an almost perfect resistor. The high-frequency resistance is inversely proportional to the DC bias current through the diode. A PIN diode, suitably biased, therefore acts as a variable resistor. The wide intrinsic region also means the diode will have a low capacitance when reverse-biased.

In a PIN diode, the depletion region exists almost completely within the intrinsic region. This depletion region is much larger than in a PN diode, and almost constant-size, independent of the reverse bias applied to the diode. This increases the volume where electron-hole pairs can be generated by an incident photon. Some photodetector devices, such as PIN photodiodes and phototransistors (in which the base-collector junction is a PIN diode), use a PIN junction in their construction.

When a PIN Diode cathode terminal is applied with positive potential in shunt configuration, the diode behaves as reverse biased and provides a short circuit

path to the RF signal to pass through without attenuation. When the PIN diode cathode terminal is applied with a negative potential, it behaves as forward biased resulting in generation of high impedance to the RF signal and does not allow it to pass through its path [12]. PIN diode basic structure is shown in Figure (2.2). Therefore, PIN diodes operates in two states i.e. forward bias or reverse bias. In

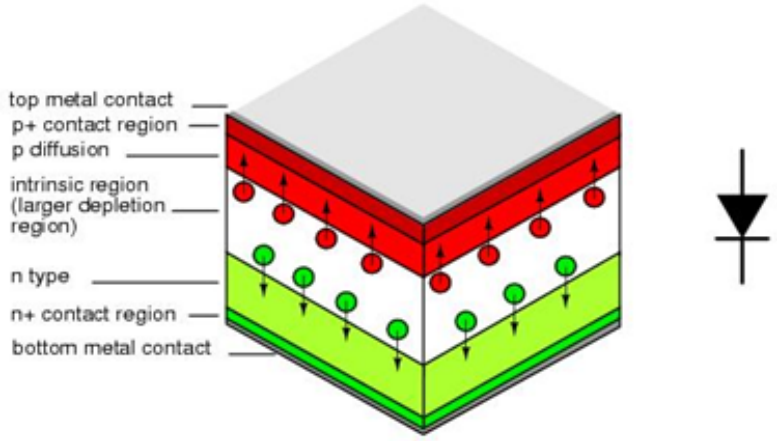

FIGURE 2.2: Structure of PIN Diode

forward biased condition, holes and electrons are injected in the intrinsic region. In case of reverse biased configuration, no charge is stored in the Intrinsic region. PIN Diode is governed by the following basic parameters.

R_p: Parallel resistance in reverse bias
C_T : Total capacitance in reverse bias condition
R_s: Series Resistance in forward bias condition
τ : Carrier lifetime
V_r: Reverse breakdown voltage of PIN diode
P_D : Average power dissipation

2.3.1 Forward biased PIN diode

The behavior of PIN diode can be easily understood by considering an inductor and resistor combination. In forward biased condition, PIN diode acts as a small resistor with a series inductor as shown in Figure (2.3). PIN diode acts like a current controlled resistor in forward bias condition and DC current passes through it resulting in accumulation of large amount of charge storage in the Intrinsic region due to electrons and hole injection in it. R_s (Series Resistance) determines the

FIGURE 2.3: Forward bias PIN Diode Model

insertion loss of PIN diode. However, it has been observed that the PIN diode has a slightly higher series resistance due to internal junction resistance because of narrow forward current [13].

$$R_s = \frac{W}{(En + Ep)I_f T}(Ohms) \tag{2.1}$$

W = Width of Intrinsic region of PIN Diode

En=Mobilization of electrons

I_f=Biased Forward Current

Ep=Mobilization of holes

T=Minority Carrier

2.3.2 Reverse Biased PIN Diode

PIN diode operates as a very high impedance during reverse bias condition, i.e Positive potential is applied to the N terminal and negative potential is applied to the P terminal. Resultantly, the intrinsic region between P and N junction increases resulting in generation of a very high impendence within a diode. The behavior of PIN diode becomes similar to the circuit with a high resistance in parallel with a capacitance. A inductance as shown in the figure 2.4 in series with resistance and capacitance also affects the circuit. The capacitance of PIN diode

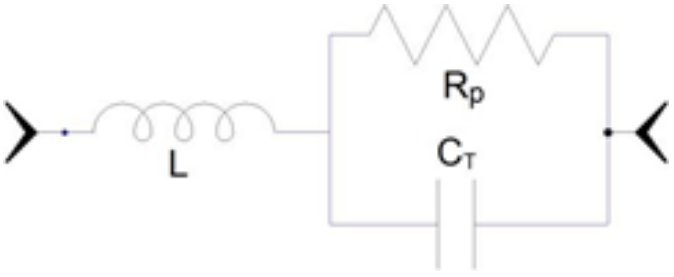

FIGURE 2.4: Model of lumped element components in reverse biased condition

model can be calculated as Co (off-state capacitance) as follows [13]:

$$C_o = \epsilon A/W \tag{2.2}$$

ϵ : dielectric constant

A : Area of diode junction

2.4 Parameters affecting the PIN Diode Switch Performance

A detailed discussion and insight into the parameters affecting the performance of PIN diodes is required to be discussed for efficient design and its subsequent operation as per the details appended below:

2.4.1 Coefficient of Voltage Reflection (Γ)

The reflection coefficient describes the amount of electromagnetic waves reflected due to impedance discontinuity in the transmission line and is the ratio of reflected wave amplitude to the incident wave.

$$\Gamma = \frac{R^-}{I^+} = \frac{(Z_L - Z_0)}{(Z_L + Z_0)} \tag{2.3}$$

The above expression describes that maximum power will be transmitted from incident transmission line to the load impedance if both are equal and resultant value of voltage reflection coefficient is zero [14].

2.4.2 Return Loss

The loss of power due to impedance mismatching between the switching elements is called as Return Loss (RL) and expressed in dBs as follows :

$$RL(dB) = -20log|\Gamma| \tag{2.4}$$

2.4.3 Voltage Standing Ratio

Voltage standing wave ratio is generally denoted by VSWR and is defined as how efficiently the RF power is transmitted from the source to the load. Voltage Standing Wave ration is expressed in terms of voltage reflection coefficient,Γ [14].

$$VSWR = \frac{V_{max}}{V_{min}} = \frac{(1 + |\Gamma|)}{(1 - |\Gamma|)} \tag{2.5}$$

The range of voltage standing wave ratio fluctuates between 1 and 0 where 1 implies that its a complete matched load with no VSWR in the circuit and vice versa.

2.4.4 Isolation

The amount of signal that can pass through the switch in On state and the amount of RF signal that can be prevented to pass through the switch in the off state is described in terms of and can be expressed as follows:

$$Isolation(dB) = (Pout)on - (Pout)off(PowerindBm) \tag{2.6}$$

An RF switch is designed keeping in consideration the isolation that is required to be maintained for keeping the signals leaking inside the undesired path. An good RF switch will provide an infinite resistance during off state thereby producing an ideal isolation between the desired and undesired paths. [10].

2.4.5 Insertion Loss

RF switches are designed keeping in consideration the insertion loss of switch during operations. It is defined as the power loss during transmission of RF signal from source to the load. It is affected by various parameters including noise, thermal and ohmic losses. The value of insertion loss is expressed in dBs. [10].

2.4.6 Power Handling

During designing of a RF switch, power handling of PIN diode is one of the most important parameters of design. Maximum power handling of PIN diode needs to be ascertained and chosen to avoid it from over-heating during operations. A number of factors determines the power handling capability of said diodes including [10].:

P_av : Average Power Handling Capability of PIN Diode

P_p : Maximum peak power dissipation

V_r : Breakdown Voltage in Reverse Bias

2.4.7 Switching speed

During forward Biased condition in series, PIN diode is switched On, whereas, in reverse biased condition the PIN diode is switched off. However, during forward biased condition in shunt configuration, PIN diode is turned Off in reverse biased condition and turned On during forward biased condition. Therefore, the switching speed determines how effectively the ON / Off procedure is done to avoid leakage. Switching speed mainly depends upon the two parameters, from forward bias to reverse bias, T_{FR}, and from reverse bias to forward bias, T_{RF}, carrier lifetime τ. The value ofT_{FR} may be calculated mathematically from the initial reverse current,I_R, and forward current,I_F, as follow [13].

$$T_{FR} = \tau log_e(1 + \frac{I_F}{I_R}) \tag{2.7}$$

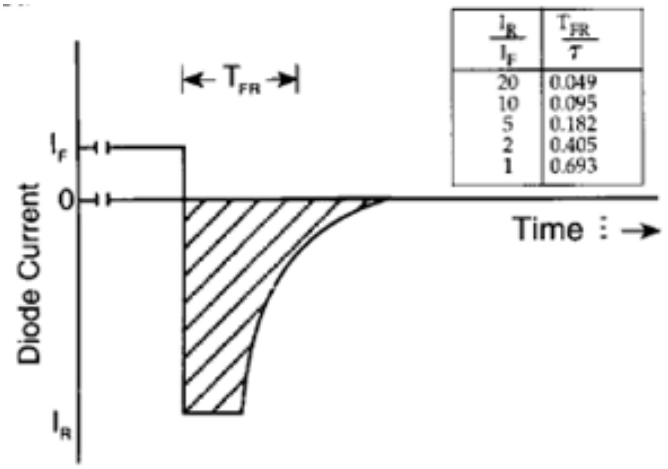

FIGURE 2.5: Characteristics of Pin Diode Switching Speed [13]

2.5 Classification of RF switches

RF switches can be classified into various configurations based on the designing technique and its utility in various applications as per the details appended below:

2.5.1 Single pole single throw series configuration (SPST)

SPST switch mainly provides On / Off switching function in a circuit and primarily used in applications requiring turning RF On & OFF. Figure (2.6) shows the series configuration of SPST switch [10]. It is used in broadband design applications which are primarily composed of DC blocking capacitors and inductors. The mathematical expressions for SPST switch can be expressed as

$$InsertionLoss(IL) = 20log(1 + \frac{R_s}{2Z_0}) \tag{2.8}$$

$$Isolation(IS) = 10log\left(1 + \frac{1}{(4fC_tZ_o)^2}\right) \tag{2.9}$$

$$P_D = \left(\frac{4R_SZ_0}{2Z_0 + R_s}\right)^2 P_av(Watts) \tag{2.10}$$

$$P_av = \frac{V_g}{4Z_0}(watts) \tag{2.11}$$

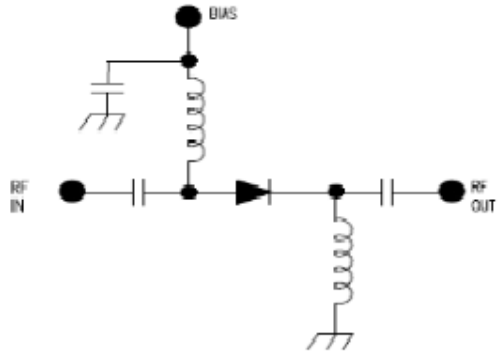

FIGURE 2.6: Single Pole Single Throw switch [10]

Where

P_av : maximum available power

P_D : Dissipation power

Rs : Series Resistance

Ct : Total Capacitance

Z_o : Inductance

2.5.2 Single Pole Single Throw shunt configuration (SPST)

For good isolation requirements at higher frequencies, PIN diode is use in shunt SPST switch configuration as shown in Figure (2.7) [10]. This configuration has small frequency bandwidth due to the use of lambda by 4 transmission lines. However, the major problem of such type of configuration is the high insertion loss due to DC blocking capacitors. The mathematical expressions for various

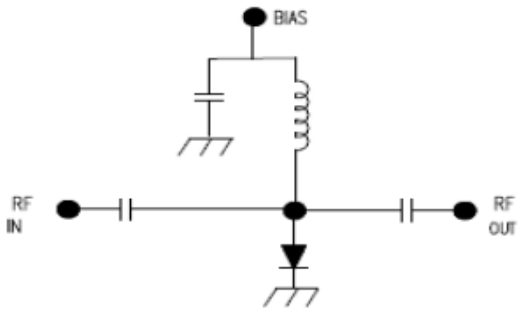

FIGURE 2.7: SPST shunt topology [10

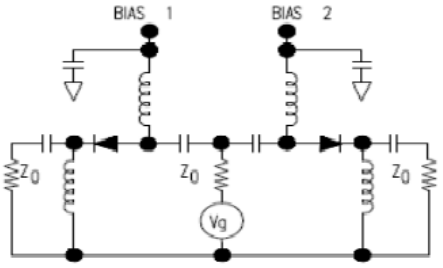

FIGURE 2.8: Series SPDT switch [10]

parameters of SPST based RF switches is appended below:

$$InsertionLossI_L = 10log(1 + (\pi f C_t Z_o)^2)dB \tag{2.12}$$

$$IsolationI_s = 20log(1 + \frac{Z_0}{2R_s})dB \tag{2.13}$$

$$P_D(forwardbiased) = 4RsZo/(Zo + 2Rs)^2 Pav(Watts) \tag{2.14}$$

$$P_D(reversebiased) = \frac{Z_o}{R_p} Pav(Watts) \tag{2.15}$$

2.5.3 Single Pole Double Throw (SPDT)

The principle of operation of single pole double throw is that the RF input is received a single port and the signal is routed through either of the two output ports available depending upon the selection criteria of SPDT switch. It is the basic building block and basis of single port multiple throw switches. It is being vast used in Radar applications during transmission from multiple antennas and during reception as well. The configuration of SPDT switch in series and shunt are shows in the following figures [10].:- Smith Chart utility provides the basic

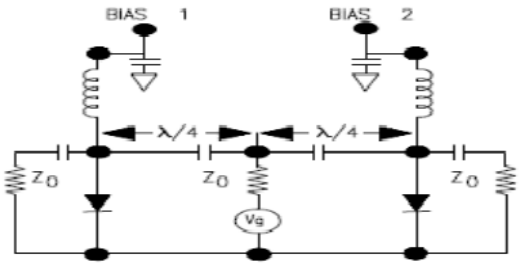

FIGURE 2.9: Shunt SPDT switch [10]

principle of series and shunt SPDT switches as it is dependent on the open /

short quarter wave transmission line theory. The basic principle of operation of series-shunt depends on the impedance transformation between the two ends of the transmission line. The two situations that are engaged in SPDT switch are appended below:

2.5.4 Open circuited quarter wave transmission line

The input impedance for the said transmission line the input impedance is appended below:

$$Z_{in} = jZ_oCot(\beta l) \tag{2.16}$$

Where β is the propagation constant and mathematically expressed as: $\beta = 2\pi\lambda$ As seen from the formula, it is evident that the input impedance of transmission line with length $\lambda/4$ is 0 which means that at input of open circuit transmission line behaves as a short circuit transmission line.

2.5.5 Short circuited quarter wave transmission Line

The input impedance for the said transmission line the input impedance is appended below

$$Z_{in} = jZ_otan(\beta l) \tag{2.17}$$

Where β is the propagation constant and mathematically expressed as; $\beta = 2\pi\lambda$ As seen from the formula, it is evident that the input impedance of transmission line with length $\lambda/4$ is infinity which means that at input of short circuit transmission line behaves as a open circuit transmission line. Therefore, it is concluded that the behavior of transmission lines can be changed into open or closed circuit by changing the biasing voltages at the input of PIN diodes.

2.6 Excitation method

Various excitation method have been constructed that can be applied to PIN diode switching circuit. For coherence and convenience, micro-strip lines are employed in the feed network of PIN diode switching circuit in the lesser gigahertz range of microwave frequency. A microstrip transmission line is a 'high' grade printed circuit structure, which consists of conductor or other track of copper on an insulating substrate. On the other side of this insulated structure, lies the 'backplane'. This plane is formed from the similar conductor employed to make transmission line [15]. The microstrip line width can be calculated as follow:

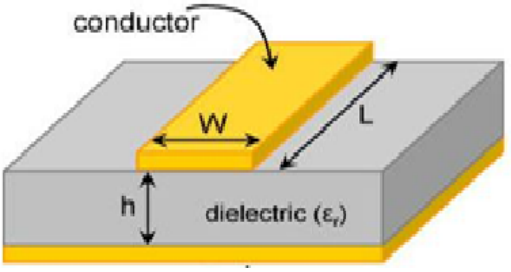

FIGURE 2.10: Geometry of microstrip transmission line

$$Z_{microstrip} = \frac{Z_o}{2\pi\sqrt{2(1+\epsilon_r)}} ln\left(1 + \frac{4h}{\omega_{eff}}\left(\frac{14+\frac{8}{\epsilon_r}}{11}\frac{4h}{\omega_{eff}} + \sqrt{\left(\frac{14+\frac{8}{\epsilon_r}}{11}\frac{4h}{\omega_{eff}}\right)^2 + \pi^2\frac{1+\frac{1}{\epsilon_r}}{2}}\right)\right) \tag{2.18}$$

Where, ω_{eff} is the effective width, which is the true width of the strip, plus a correction to account for the non-zero thickness of the conductor. The effective width is given by:

$$\omega_e ff = \omega + t\frac{1+\frac{1}{\epsilon_r}}{2\pi} ln\left(\frac{4\epsilon_r}{\sqrt{\left(\frac{t}{h}\right)^2 + \left(\frac{1}{\pi}\frac{1}{\frac{W}{t}+\frac{11}{10}}\right)^2}}\right) \tag{2.19}$$

Z_o= Characteristic impedance

ϵ_r=Dielectric constant of medium

w=Conductor width

h= Substrate Thickness

t= Conductor Thickness

The characteristic impedance Z_0 is also a function of the ratio of the height to the width w/h (and ratio of width to heighth/w) of the transmission line. According to Bahl and Trivedi I. [17], the characteristic impedance Z_0 of microstrip is calculated by:

when= $(\frac{w}{h}) < 1$

$$Z_0 = \frac{60}{\sqrt{\omega_{eff}}} ln\left(8\frac{h}{w} + 0.25\frac{w}{h}\right)(ohms) \tag{2.20}$$

when= $(\frac{w}{h}) \geq 1$

$$Z_0 = \frac{120\pi}{\sqrt{\omega_{eff} \times \left[\frac{w}{h} + 1.393 + \frac{2}{3} ln\left(\frac{w}{h} + 1.44\right)\right]}}(ohms) \tag{2.21}$$

This equation is helpful in order to roughly calculate the width of microstrip line matched to the port.

2.7 Summary

In this chapter, different RF switching techniques have been discussed briefly. Advantages, features and applications of PIN diode make it very versatile and excellent choice for a designer to use in the development of efficient RF Switch. In addition, the PIN diode switching circuit properties are explained so the reader can understand the behavior of PIN diode switching circuit.

Chapter 3

LITERATURE REVIEW

This section provides a synopsis of single port double throw RF switches based on PIN diode and its technological trends presented in literature.

3.1 Design and Analysis of Broadband High Isolation of Discrete Packaged PIN Diode SPDT Switch

In this paper [16], three different topologies are discussed for designing of SPDT switch along with description of impact on isolation and insertion loss in each design. A good design of SPDT switch depends on low insertion loss, high isolation, small circuit size and low operation current. SPDT circuit topologies i.e. (i) single-shunt switch (Figure 3.1) (ii) series-shunt switch (Figure 3.2) and (iii) series-shunt-shunt switch (Figure 3.3)are compared in [16] for better isolation performance in OFF state.

The insertion loss of this single-shunt PIN diode design topology depends on its junction capacitance and isolation depends on its series resistance. Therefore, this circuit topology gives good isolation results.

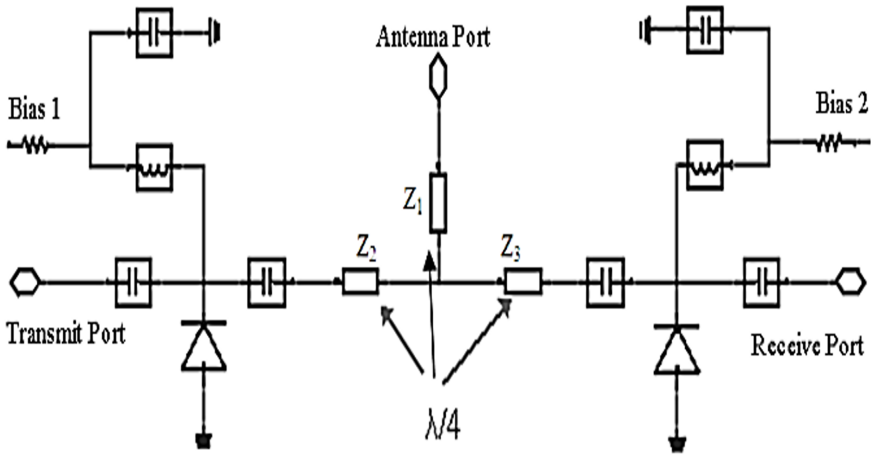

FIGURE 3.1: Single-shunt switch topology [16]

The second design topology i.e series-shunt switch topology achieves better isolation than single shunt design due to impact of isolation resulted from single shunt and single series diode. However, the complexity of the biasing circuit increases due to said configuration. The series-shunt-shunt topology has one series and tow

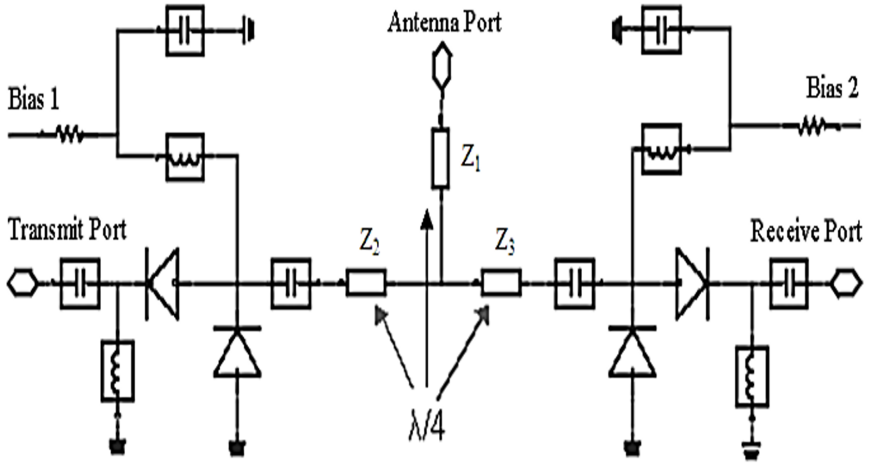

FIGURE 3.2: Series-shunt topology [16]

shunt PIN diodes which results in improving the isolation by 6dB. Therefore, the same is used in this paper for simulation and fabrication for 0.5GHz to 4 GHz. This design gives minimum insertion loss of 2.2 dB with isolation of 25 dB at frequency of 1$\tilde{2}$ GHz. However, the switch is designed, simulated and tested on a very little power of 15 dBm and no constraints on size of RF switch is presented in this design.

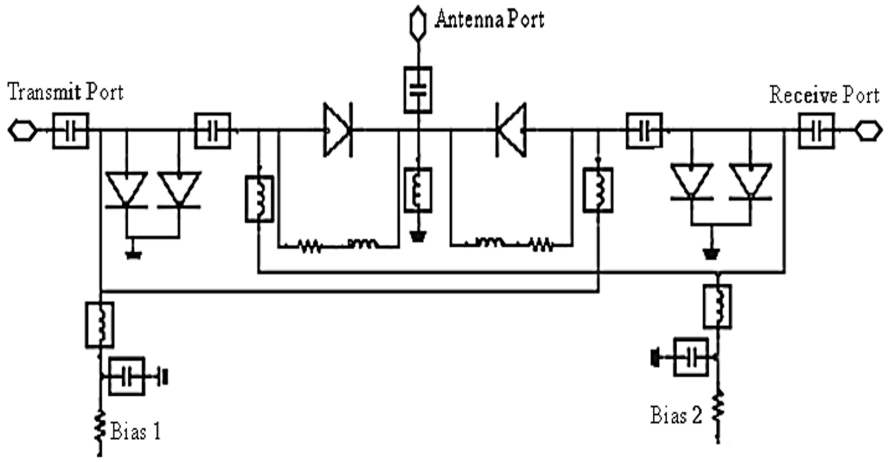

FIGURE 3.3: Series-shunt-shunt topology [16]

3.2 PIN Diode Modeling for Simulation and Development of High Power Limiter

An RF switch is presented in this paper [17] based on PIN diode modelling for switching applications. The design revolves around the improvement in isolation and insertion loss of SPDT switch by considering the parameters of forward resistance and off state capacitance of PIN diodes. The OFF state capacitance affects the isolation of the circuit in reverse biased condition of PIN diodes, whereas, the forward resistance affects the insertion loss of the circuit in forward biased condition.

The high Isolation has been achieved by using a resonant LC circuit in parallel with the PIN diode in order to overcome the affect of small RF leakage through PIN diode in OFF state condition (Figure 3.4). The LC circuit in parallel provides a band stop response and provides even higher impedance to RF signal. This design gives minimum insertion loss of 0.94dB with maximum isolation of 41 dB over 1.5-3.5GHz frequency band. However, the switch is designed, simulated and tested on a very little power of 10 dBm and no constraints on size of RF switch is presented in this design.

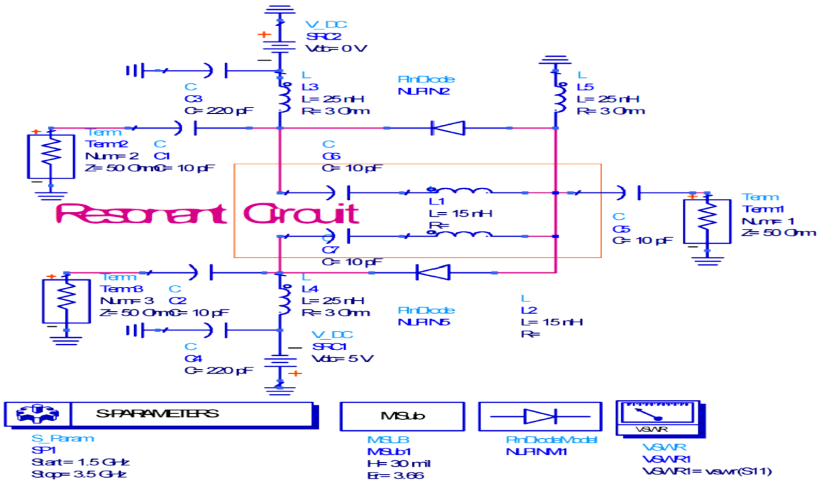

FIGURE 3.4: LC Resonant Circuit [17]

3.3 Design Comparison of RF SPDT Switch with Switchable Resonators

A comparison of RF SPDT switches has been presented in this paper [18]. Four RF SPDT switch designs have been compared keeping in consideration the size, isolation, return loss, insertion loss, number of utilized PIN diodes. In design 1 (Figure 3.5), SPDT switch with two cascaded switchable transmission line stub resonators was demonstrated. In this this design, the circuit size is 1260 mm isolation is 36 dB insertion loss is 1.46 and return loss is 1.80 dB. In design 2

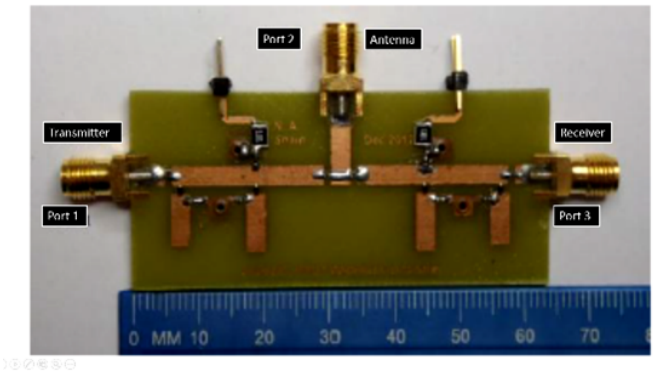

FIGURE 3.5: SPDT Design 1 [18]

(Figure 3.6), SPDT switch with two cascaded switchable radial stub resonators was demonstrated. In this this design, the circuit size is 1260 mm isolation is 38.67 dB insertion loss is 1.71 dB and return loss is 2.02 dB. In design 3(Figure 3.7),

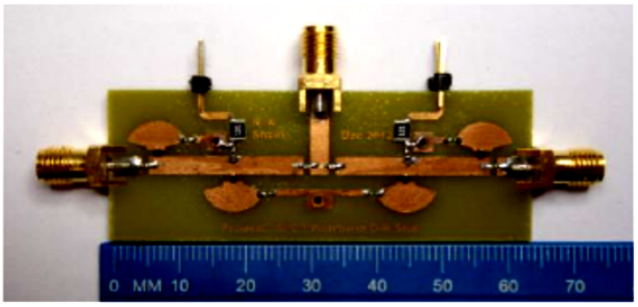

FIGURE 3.6: SPDT Design 2 [18]

SPDT switch with a three-cascaded switchable parallel coupled lines and single radial stub resonator was demonstrated. In this this design, the circuit size is10120 mm isolation is 41.83 dB insertion loss is 2.68 dB and return loss is 18.03 dB.

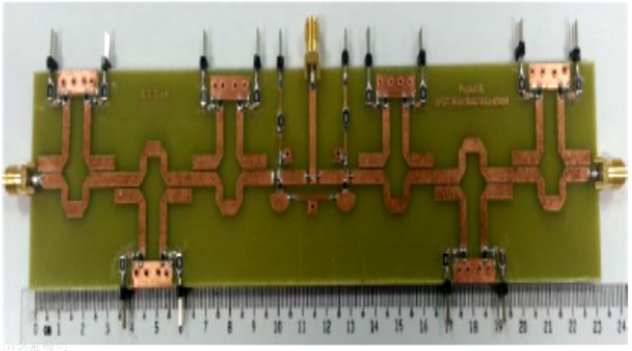

FIGURE 3.7: SPDT Design 3 [18]

In design 4(Figure 3.8), SPDT switch with three cascaded switchable rings and single radial stub resonator two cascaded switchable transmission line stub resonators was demonstrated. In this this design, the circuit size is 7776 mm isolation is 33.51 dB insertion loss is 1.96 dB and return loss is 23 dB.

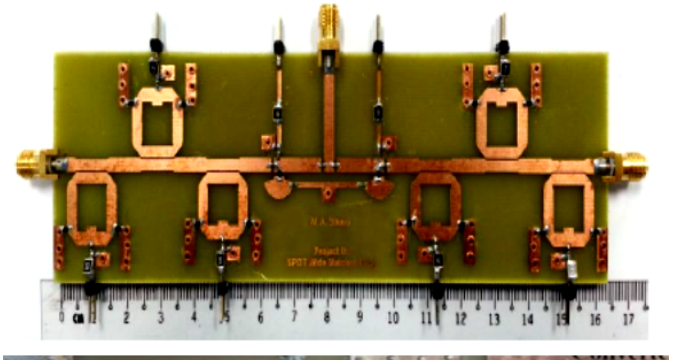

FIGURE 3.8: SPDT Design 4 [18]

The four design has been compared in this paper with description of insertion loss and isolation of each detailed design. The constraints of size of RF SPDT switches were discussed in detail, however, since these are only tested for LTE and WiMax technologies, therefore, the power handling capability of these RF switches is around 15 dBm maximum.

3.4 Design and Analysis of PIN Diode SPDT Switch and Feeding Circuit for Pulse Doppler Radar

The paper[19] presents design, analysis and performance of PIN Diode base RF switch in L band at a frequency of 1200 MHZ. The paper presents the different techniques of designing the SPDT switch and used Shunt-Shunt switch topology for better isolation between transmit and receive paths. Two quarter wave length sections were chosen each terminated on shunt diodes. $\lambda/2$ transmission lines are attached to each PIN diode before the ground to assist in minimizing mismatch losses. Additional Diodes and $\lambda/4$ lines are added at each stage to improve the isolation of the circuit. The design was simulated in Advanced Design system Software and fabricated on FR4 substrate. Figure (3.7) shows fabricated SPDT switch based pulse generator designed for 1.2 to 1.25GHz frequency range. This design gives minimum insertion loss of 2.1 dB with maximum isolation of 40 dB on 1.2 1.25 GHz frequency band. However, the switch is designed, simulated and tested on a very little power of 15 dBm and no constraints on size of RF switch is presented in this design.

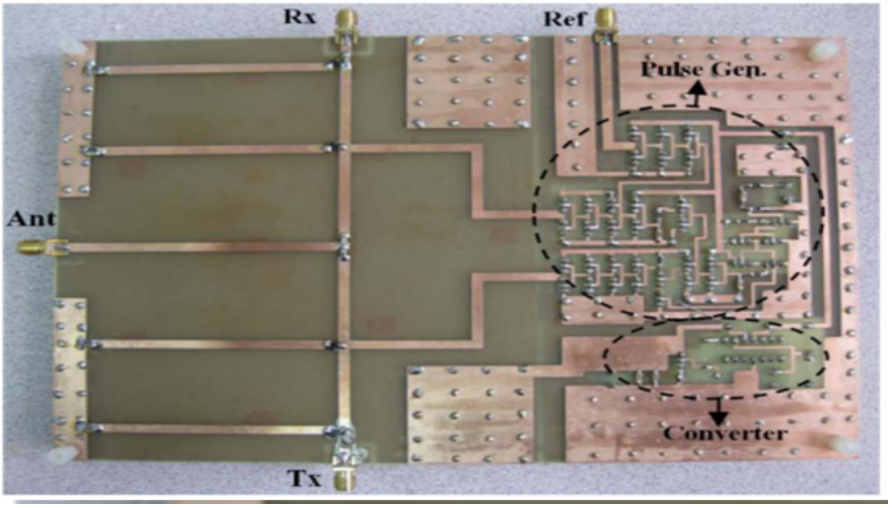

FIGURE 3.9: Assembled low cost T/R module [19]

3.5 Power Handling Capability of Microstrip Line

A detailed analysis for calculating the power handling capability of micro strip lines is discussed in this paper[20]. It describes that the power handling capability of microstrip lines is limited due to the factors including heating caused by ohmic and dielectric losses. The average power handling capability is limited due to increase in temperature in conductor and its dielectric losses. Where-as the peak power handling capability is limited due to breakdown between the strip conductor and ground plane. The parameters which affect the average power handling capabilities of microstrip line includes

(a) Transmission lines losses

(b) Thermal conductivity of the substrate material

(c) Surface area of the the strip conductor

(d) Ambient temperature

A typical microstrip line is shown in the above figure in which
h = Substrate thickness
t = Strip Conductor Thickness

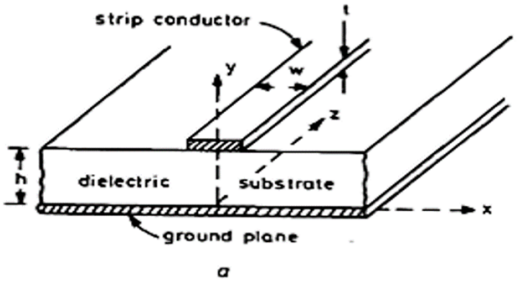

FIGURE 3.10: Microstrip Substrate

W = Strip Conductor Width

The following relation can calculate the average power handling capability

$$P_a v = (T_{max} - T_{amb})/\Delta T \tag{3.1}$$

ΔT= Rise in Temperature per Watt

T_{max}=Maximum Operating Temperature

T_{amb}= Ambient Temperature

The rise in temperature is given by the following relation

$$\Delta T = \frac{h}{K}\left(\frac{\Delta P_e}{W_e} + \frac{\Delta P_d}{2W_{eff}}\right) \tag{3.2}$$

Where K = Thermal Conductivity of Substrate

h = Thickness of strip conductor

$$\Delta P_e = 1 - e^{(-0.2303\alpha_c)} \tag{3.3}$$

Where $\alpha_c \left(\frac{dB}{m}\right)$ is the attenuation coefficient due to loss in the conductor strip

Calculation of attenuation coefficient due to conductor strip given by the relation

$$\alpha_c \left(\frac{dB}{m}\right) = \frac{8.686 R_s}{Z_o W} \tag{3.4}$$

$$R_s = \sqrt{\frac{\pi f \mu_o}{\sigma}} \tag{3.5}$$

$$\Delta P_d = 1 - e^{(-0.2303\alpha_d)} \tag{3.6}$$

$\alpha_d \left(\frac{dB}{m}\right)$ is the attenuation coefficient due to dielectric loss
The relation gives calculation of attenuation coefficient due to dielectric loss

$$\alpha_d \left(\frac{dB}{m}\right) = \frac{27.3\sqrt{\epsilon_r} tan\delta}{\lambda_o} \tag{3.7}$$

$$W_e = \frac{120\pi h}{Z\sqrt{\epsilon}} \tag{3.8}$$

Where ϵ =effective relative permittivity

$$W_{eff} = W + \frac{W_{eff}(0) - W}{1 + (f/f_p)} \tag{3.9}$$

where

$$f_p = \frac{Z}{2\mu h} \tag{3.10}$$

$$W_{eff}(0) = \frac{377h}{Z\sqrt{\epsilon}} \tag{3.11}$$

3.6 Gap Analysis

A comparison of various parameters of SPDT switches discussed in this chapter is tabulated for analysis. It can be concluded from the tabular comparison table 3.1 that the literature is focused either on the miniature design with low power requirements, or designing of RF switches without space limitations keeping in considerations isolation and insertion loss as a paramount bench mark. The

Reference	Insertion Loss	Isolation	Power Handling Capability	Size	Remarks
Unit	(dB)	dB	dBm	mm^2	
Para 3.1	2.2	25	15	-	No size constraints defined in design
Para 3.2	0.94	41	10	-	
Para 3.3 (a)	1.46	36	23	1260	
(b)	1.71	38.67	23	1260	
(c)	2.68	41.38	23	10120	
(d)	1.96	33.51	23	7776	

TABLE 3.1: Comparison of Performance Parameters

miniaturized design requirements along with capability of high power handling were not demonstrated / discussed. Therefore, designing and simulation of an RF SPDT switch capable of handling high power designed within a miniaturized design generates a new perspective for designing a miniaturized high power RF SPDT switch.

3.7 Summary

This chapter gives an overview of different technological developments for designing and fabrication of single port double through switches using PIN diodes. The parameters of paramount importance including insertion loss, isolation, power handling capability within different sizes has been discussed in detail. The literature survery shows that there is a trade off between insertion loss and isolation along with trade off between performance and the size of SPDT switches. In addition the literature review discusses the ways of calculating the power handling capability for various substrate materials that can be used to evaluate the power handling capability of an SPDT switch. This chapter gives an overview of different technological developments for designing and fabrication of single port double through switches using PIN diodes. The parameters of paramount importance including insertion loss, isolation, power handling capability within different sizes has been discussed in detail. The literature survery shows that there is a trade off between

insertion loss and isolation along with trade off between performance and the size of SPDT switches. In addition the literature review discusses the ways of calculating the power handling capability for various substrate materials that can be used to evaluate the power handling capability of an SPDT switch.

Chapter 4

DESIGN, SIMULATIONS AND MEASUREMENTS

4.1 Introduction

In this chapter, design approach and its utilization in the development of miniaturized SPDT RF switch is discussed briefly. Advanced Design system (ADS) 2016 from Agilent is used to validate the design parameters and the working principle of proposed design. With the help of simulation results, it is proved that the proposed design is capable of withstanding high power requirements despite having small size and provides good isolation between the two antennas with minimum degradation in insertion loss. The simulation results were further compared with actual values after fabrication of SPDT RF switch using Vector Network Analyzer from Rohde and Schwarz.

4.2 Design Methodology

To achieve the targeted result of miniaturized high power SPDT switch, following design methodology was adopted keeping in consideration the various technical aspects as described in subsequent paragraphs.

4.2.1 Miniaturized Design Dependency

The miniaturized design concept required in-depth analysis and simulations of various factors before finalization. The design requirements of target SPDT switch revolves around the selection of RF switching techniques / philosophy in combination with selected material keeping in consideration the following major challenges:

1. Limited Space Availability
2. High Power Requirement (60 dBm)
3. Good Performance (Insertion Loss, Isolation & Return Loss)

4.2.2 RF Switching Methodology

The foremost requirement of the design is selection of suitable technique keeping in consideration the design requirements and literature review. As discussed earlier in chapter 2, PIN diode based switching has the capability of high power handling despite having smaller size, low series resistance, high parallel resistance and low junction capacitance. With selection of switching methodology, series-shunt SPDT switch based design is selected that works on the principle of open and shorted quarter wave transmission line theory. The transformation of impedance between the two ends of the transmission line is the fundamental concept used in these switches.

4.2.3 Factors for Power Handling Capability

Designing phase of miniaturized SPDT switch with capability of high power handling not only demands a well-structured design, but also requires appropriate selection of substrate material capable of handling high RF power within limited space. This step is handled by dividing it into two broader categories:-

1. Study of Substrate

   The substrate material is selected keeping in consideration the design factors vis a vis availability of RF sheets in the market.

2. Substrate Material Selection

   Simulations were done using ADS tools to find out the best substrate capable of designing SPDT switch in limited space availability. Moreover, Power handling capability of RF transmission lines has been discussed in detail.

4.2.4 Simulations

ADS 2016 was used for designing of SPDT switch. Following methodology was adopted during designing phase and getting the simulated results

- Designing of basic SPDT architecture in ideal environment
- Iterative simulations by varying different parameters including change in impendences of RF transmission lines and addition / deletion of RF transmission lines
- Getting desired performance results in case of ideal scenario
- Simulation in ADS software by adding parameters of selected substrate and components to have a real environment simulated view
- Designing of RF SPDT layout in ADS
- Consideration of physical requirements of design during switch design
- Analysis of Co-simulation results in ADS

4.2.5 Fabrication of Design

After achieving the desired results, the fabrication of SPDT switch was undertaken on selected substrate material. SPDT switch was tested using Vector Network Analyzer and the results were compared with the simulation results.

4.3 Functionality of Proposed SPDT Switch

Figure (4.1) presents the overall schematic of the Proposed SPDT switch designed by using combination of PIN diodes in a shunt SPDT switching topology.

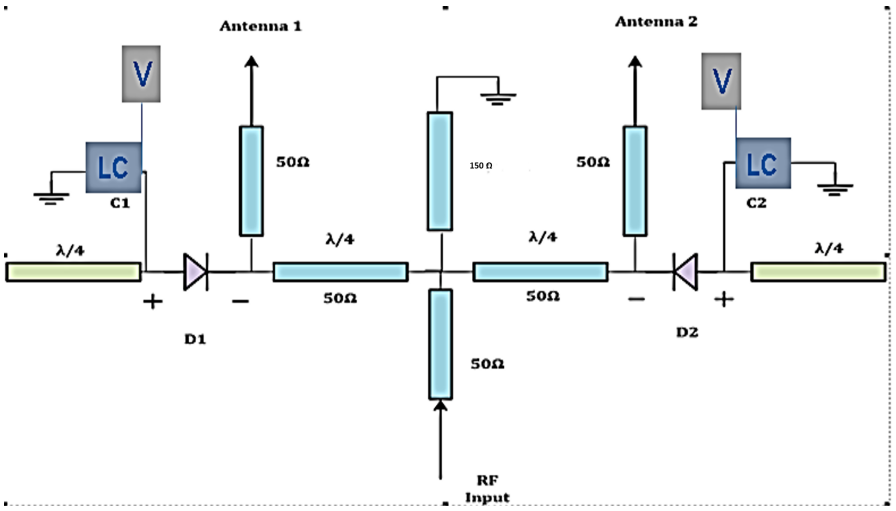

FIGURE 4.1: Functional block diagram of proposed SPDT switch

4.3.1 Working principle

The working principle depends on the connectivity of transmission lines in configuration of open circuit or short circuit. The transmission lines can be made short circuit or left open circuited by applying the different biasing voltages to the PIN diodes. A detailed analysis of working methodology of transmission line reveals that transmitting signal is controlled by the PIN diodes to the respective ports through change in its biasing voltages.

When the biasing voltage at anode terminal of D1 is at low potential and at anode terminal of D2 is high potential, D1 will become reverse biased and the transmission will be done through antenna 1. At the same time D2 is forward biased and will present an open-circuit to input RF. This results in transformation of the transmission line at the input of diode D2 into high impedance transmission

line. Due to the symmetry, same technique is applied when transmitter transmits power from antenna 2.

Working functionality of proposed design is tabulated in table 4.1.

FUNCTION	**D1**	**D2**
Transmission from Antenna 1	OFF	OFF
Transmission from Antenna 2	ON	ON

TABLE 4.1: Working functionality of proposed design

4.3.2 Proof of Concept

The schematic of the proposed SPDT topology is shown in Figure (4.2). It is worth mentioning that ideal transmission lines are used for the proof of concept. When applying low potential -50 V at anode terminal of Pin diode 01 (NLPIN3) it becomes reverse biased and presented open circuit on transmission line to the coming signal. At this instant, Pin Diode02 is forward biased by applying high potential +12V on its anode terminal so that signal may travel from port 1 to port 2. C3 and C4 capacitors are used as decoupling capacitors for filtering DC voltages. TL6 and TL10 are RF Chokes used to isolate DC from RF. TL7 and TL11 are 35-ohm open circuited transmission lines, which are used to narrow down the bandwidth. TL1, TL2 , TL3, TL4, TL5 and TL11 are 50-ohm transmission lines.

Simulated results of proposed shunt topology are shown in Figure (4.3). It is evident from Figure (4.3) that the design of SPDT switch achieved an ideal insertion loss of negligible value and high isolation between the ports. The proof of concept is finalized and parameters related to substrate, pin diode specifications etc are required to be added to have a real picture from simulations. The iterative process was used to get the results, as it was observed that increasing the ohmic value of transmission line TL7 and TL 11 results in increase in the isolation / insertion loss values.

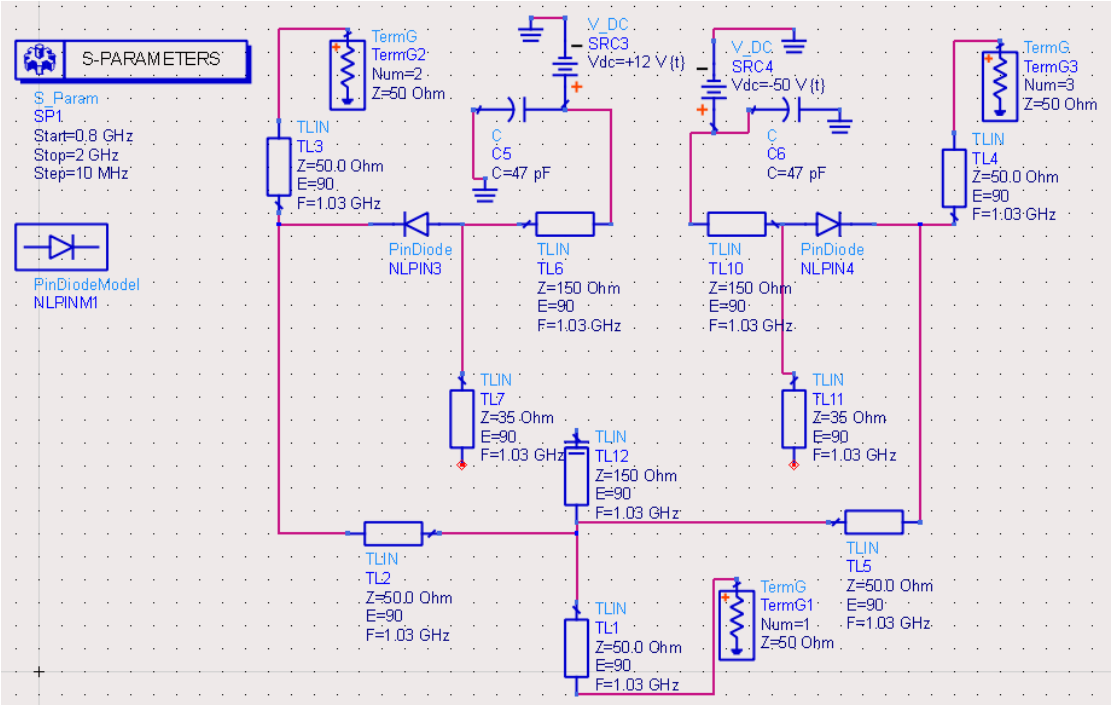

FIGURE 4.2: Schematic of proposed SPDT topology in ADS

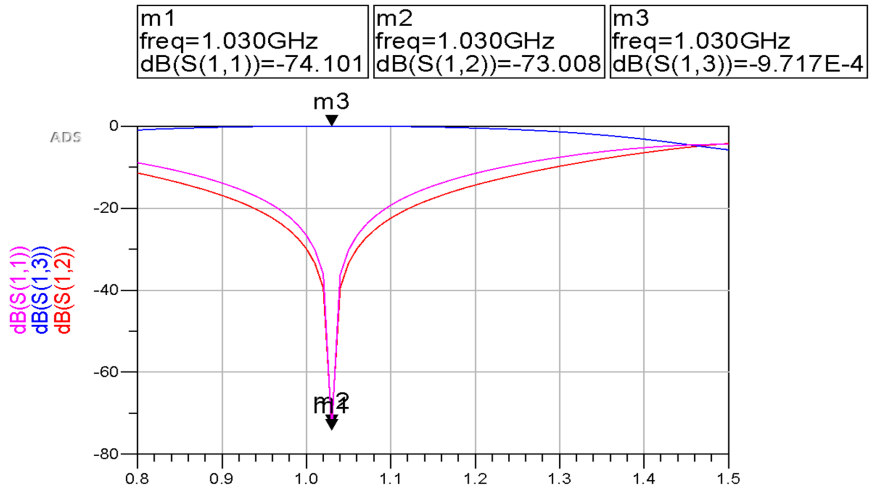

FIGURE 4.3: Insertion loss proposed SPDT during transmission from port 3

4.4 Substrate Selection

Following two substrate materials were selected for comparison due to their ready availability and their vast usage in designing for RF Aviation products due to its Mil standard specifications:

(a) FR4

(b) Rogers RT Duroid 6010.2 LM

A side by side comparison of basic parameters of both the substrate materials are appended in table 4.2[23] [24].

Material	**Rogers RT Duroid 6010.2LM**	**FR4**
Dielectric constant	10.2	4.4
Substrate Thickness	0.635 mm	0.8 mm
Loss Tangent	0.0023	0.014
Copper Thickness	35um	35um
Thermal Conductivity	0.86 W/(m.C)	0.25 W/(m.C)

TABLE 4.2: Basic Parameters of Substrate Material

4.4.1 Power Handling Capability of FR4

As discussed in Chapter 3, a detailed analysis of power handling capability of FR4 material has been elaborated:

Thermal conductivity $K = 0.25W/m.C$

Characteristic Impedance $Z = 50\Omega$

Operating frequency $f = 1030MHz$

Thickness of sheet $h = 0.0008meters$

Dielectric Constant $\epsilon_r = 4.4$

Width for 50Ω transmission line $W = 0.00148m$

Loss tangent for FR4 $\tan\delta = 0.013$

Relative permittivity $\mu_o = 4\pi * 10^{-7}$

The average power handling capability of FR4 can be calculated by the using equations 3.1 to 3.11 as per the following details:

Calculation of attenuation coefficient due to conductor strip given by the relation.

$$\alpha_c \left(\frac{dB}{m}\right) = \frac{8.686R_s}{Z_o W} \tag{4.1}$$

$$R_s = \sqrt{\frac{\pi f \mu_o}{\sigma}} \tag{4.2}$$

Putting the values in the above equations results $R_s = 0.0082$ Putting the value in equation 4.1

$$\alpha_c \left(\frac{dB}{m}\right) = 0.96 \tag{4.3}$$

The relation gives calculation of attenuation coefficient due to dielectric loss

$$\alpha_d \left(\frac{dB}{m}\right) = \frac{2.73\sqrt{\epsilon_r}\tan\delta}{\lambda_o} \tag{4.4}$$

$$\alpha_d \left(\frac{dB}{m}\right) = 2.48 \tag{4.5}$$

Total attenuation coefficient due to die electric loss is

$$\alpha_c \left(\frac{dB}{m}\right) + \alpha_d \left(\frac{dB}{m}\right) = 0.96 + 2.48 = 3.44 \tag{4.6}$$

Since rise in temperature in degree Celsius per unit watt is given by the following relation

$$\Delta T = \frac{h}{K}\left(\frac{\Delta P_e}{W_e} + \frac{\Delta P_d}{2W_{eff}}\right)\frac{C^o}{Watt} \tag{4.7}$$

Where

$$\Delta P_c = 1 - e^{(-0.2303\alpha_c)} \tag{4.8}$$

$$\Delta P_c = 0.198 \tag{4.9}$$

And

$$\Delta P_d = 1 - e^{(-0.2303\alpha_d)} \tag{4.10}$$

$$\Delta P_d = 0.435 \tag{4.11}$$

Where

$$W_e = \frac{120\pi h}{Z\sqrt{\epsilon}} \tag{4.12}$$

and

$$W_{eff} = W + \frac{W_{eff}(0) - W}{1 + (f/f_p)^2} \tag{4.13}$$

where

$$f_p = \frac{Z}{2\mu h} = 2.48 * 10^{10} \tag{4.14}$$

$$W_{eff}(0) = \frac{377h}{Z\sqrt{\epsilon}} = 0.0028 \tag{4.15}$$

$$W_{eff} = W + \frac{W_{eff}(0) - W}{1 + (f/f_p)^2} \tag{4.16}$$

$$W_{eff} = 0.0027 \tag{4.17}$$

Putting values in main equation to calculate change in temperature per unit watt

$$\Delta T = 0.483\frac{C^o}{Watt} \tag{4.18}$$

If the maximum operating temperature is 100 C^o and ambient temperature is 25 C^o Then the average power handling is

$P_{av} = (T_{max} - T_{amb})/\Delta T$

$P_{av} = (100 - 25)/0.483$

$$P_{av} = 154.21Watts \tag{4.19}$$

4.4.2 Power Handling Capablity of Rogers 6010.2LM

The detailed analysis of Average Power Handling Capability of Rogers 6010.2 LM is appended below: Thermal conductivity $K = 0.78W/m.C$

Characteristic Impedance $Z = 50\Omega$

Operating frequency $f = 1030MHz$

Thickness of sheet $h = 0.000635meters$

Dielectric Constant $\epsilon_r = 4.4$

Width for 50Ω transmission line $W = 0.000533m$

Loss tangent for FR4 $\tan\delta = 0.0023$

Relative permittivity $\mu_o = 4\pi * 10^{-7}$

The average power handling capability of roger can be calculated by the using equations 3.1 3.11 as per the following details:-

Putting the values in the equations (3.4) and (3.5) results

$$R_s = 0.00825 \tag{4.20}$$

$$\alpha_c \left(\frac{dB}{m}\right) = 0.96 \tag{4.21}$$

Putting the values in equation (3.6)

$$\alpha_d \left(\frac{dB}{m}\right) = \frac{2.73\sqrt{\epsilon_r}\tan\delta}{\lambda_o} \tag{4.22}$$

$$\alpha_d \left(\frac{dB}{m}\right) = 0.668 \tag{4.23}$$

Total attenuation coefficient due to die electric loss is

$$\alpha_c \left(\frac{dB}{m}\right) + \alpha_d \left(\frac{dB}{m}\right) = 2.68 + 0.668 = 3.348 \tag{4.24}$$

Since rise in temperature in degree Celsius per unit watt is given by the following equation (3.2)

$$\Delta T = \frac{h}{K}\left(\frac{\Delta P_e}{W_e} + \frac{\Delta P_d}{2W_{eff}}\right)\frac{C^o}{Watt} \tag{4.25}$$

$$\Delta P_c = 1 - e^{(-0.2303\alpha_c)} \tag{4.26}$$

$$\Delta P_c = 0.46 \tag{4.27}$$

and

$$\Delta P_d = 1 - e^{(-0.2303\alpha_d)} \tag{4.28}$$

$$\Delta P_d = 0.142 \tag{4.29}$$

Where

$$W_e = \frac{120\pi h}{Z\sqrt{\epsilon}} \tag{4.30}$$

and

$$W_{eff} = W + \frac{W_{eff}(0) - W}{1 + (f/f_p)^2} \tag{4.31}$$

where

$$f_p = \frac{Z}{2\mu h} = 3.13 * 10^{10} \tag{4.32}$$

$$W_{eff}(0) = \frac{377h}{Z\sqrt{\epsilon}} = 0.0015 \tag{4.33}$$

$$W_{eff} = W + \frac{W_{eff}(0) - W}{1 + (f/f_p)^2} \tag{4.34}$$

$$W_{eff} = 0.0015m \tag{4.35}$$

Recalling equation 3.2 and Putting values in main equation to calculate change in temperature per unit watt.

$$\Delta T = 0.288 \frac{C^o}{Watt} \tag{4.36}$$

f the maximum operating temperature is 100 C^o and ambient temperature is 25 C^o Then the average power handling is

$$P_{av} = (T_{max} - T_{amb})/\Delta T \tag{4.37}$$

$$P_{av} = 260.70 Watts \tag{4.38}$$

It can be concluded that the Roger Substrate 6010.2 LM is capable of handling the high average power as compared with FR4. Moreover, the attenuation loss of Roger Substrate is also less as compared with the FR4, therefore, Roger substrate 6010.2 LM is most suitable for usage in the SPDT switch. Since the average power required to be handled by the component depends upon the duty cycle, therefore, an SPDT switch with a peak power of 1 Kw can handle a duty cycle of more than 10 percent (100 watt) keeping in consideration the above mentioned calculations.

4.4.3 Miniaturization Analysis of Substrates

To undertake the final selection of substrate, corresponding design in terms of dimensions was analyzed. ADS tool Line calculator (Figure 4.4)was used to ascertain the effectiveness of design vis a vis its miniaturization. Line Calc Tool uses the technical parameters of substrates and finally displays the corresponding

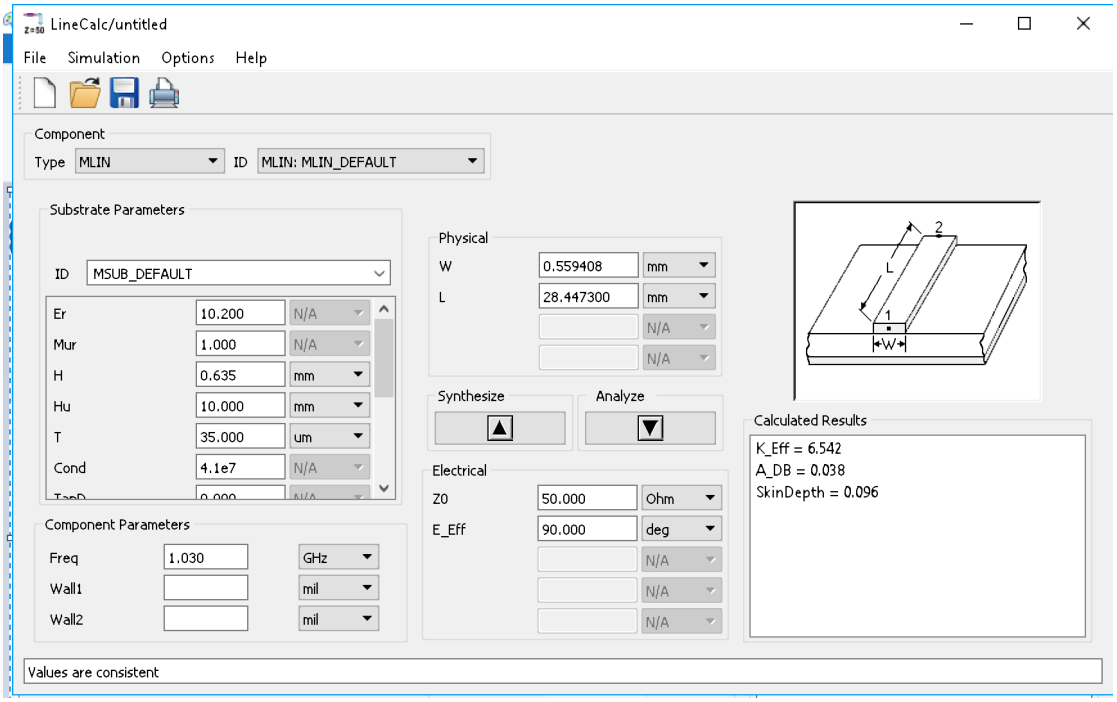

FIGURE 4.4: Line Calc Tool

physical dimensions as per requirements. Same tool was used by putting in the values of FR4 and Rogers 6010.2 LM substrate and following analysis is done:

(a) A 35 ohm transmission line of proposed SPDT RF switch was simulated on FR4 substrate resulting in achieving an RF patch of length 40 mm and width of 2.59mm on FR4 substrate material.

(b) A 50 ohm transmission line of proposed SPDT RF switch was simulated on FR4 substrate resulting in achieving an RF patch of length 40 mm and width of 1.484mm on FR4 substrate material.

(c) A 35 ohm transmission line of proposed SPDT RF switch was simulated on Rogers RT Duroid 6010.2LM substrate resulting in achieving an RF patch of length 27 mm on substrate material with a width of 0.812 mm.

(d) A 50 ohm transmission line of proposed SPDT RF switch was simulated on Rogers RT Duroid 6010.2LM substrate resulting in achieving an RF patch of length 27 mm and width of 0.533 mm on substrate material

Since the major objective is to achieve the miniaturization, Rogers 6010.2LM is selected for the design keeping in consideration the results achieved in the previous paragraphs. The next major step is to verify the capability of said substrate for effective handling of high RF power.

4.5 Design specification

Microsemi PIN diode UM6204E is used for switching configuration of this design. The thermal resistance of this low loss PIN diode is considerable small due to symmetrical thermal paths. The main reason for using this PIN diode is its capability to carry high power with low series resistance, high parallel resistance and low junction capacitance [25]. As shown in Table 4.3, capacitors are used in combination as a decoupling capacitor for filtering biasing voltages of each PIN diode and its specifications are provided in Appendix-B.

Parameter	**Value/Model**
Pin Diode	UM6204E
Capacitor	08052U470FAT2A
	(47pF)
Voltage Sources	-50V, +12V

TABLE 4.3: Resources used in design

4.5.1 Specification of UM6204E

UM6204E	
Frequency Range	0.1-1500 MHz
Series Resistance (Rs)	0.5ohm
Parallel resistance (Rp)	1Kohm
Total capacitance	1pF
Reverse Breakdown Voltage	400V

TABLE 4.4: Specification of UM6204E

The Spice Model values of pin diode UM6204E provided by the manufacturer are mentioned in Table 4.5.

Part #	Parameter	Description	Value	Unit
UM6204E	IS	Saturation Current	1.0 E-14	Amps
	BV	Breakdown Voltage	425	Volts
	WI	I region Width	9.6 E-5	Meters
	Rr	I-region Reverse Bias Resistance	1 E+5	Ω
	TAU	Ambipolar I-region Lifetime	5.0 E-6	Sec
	Rs	Ohmic Resistance = Rc + Rj	0.05 + Rj (I)	Ω
	CJ0	Junction Capacitance @ 0V	7.0 E-13	Farads
	Vj	Junction Potential	0.70	Volts
	M	Grading Coefficient	1.0	None
	KF	Flicker Noise Coefficient	0	None
	AF	Flicker Noise Exponent	1.0	None
	FC	Forward Bias Depletion Capacitance Coefficient	0.5	None
	FFE	Flicker Noise Frequency Exponent	1.0	None

TABLE 4.5: The Spice Model values of PIN diode UM6204E

4.5.2 Schematic design on Rogers6010.2 LM substrate in ADS2016

After taking preliminary steps of analyzing the proposed ideal SPDT design, selection of substrate, selection of components, the next major step is the simulation as a complete package in ADS. ADS has the capability of simulation of complete design by including factors of substrate properties, diode and capacitors specifications. Frequency sweep is set from 800MHz to 1500MHz with 1MHz step size as shown in Figure (4.5). Figure (4.5) shows the schematic design involving the details of the substrates and actual length & width calculated using line calculator tool of ADS keeping in consideration the design parameters. It includes the simulated width of each transmission line, the actual parameters of the substrate and pin diode spice model. Its results are appended: It has been observed that after including the details of substrates and actual dimensions, the results of isolation

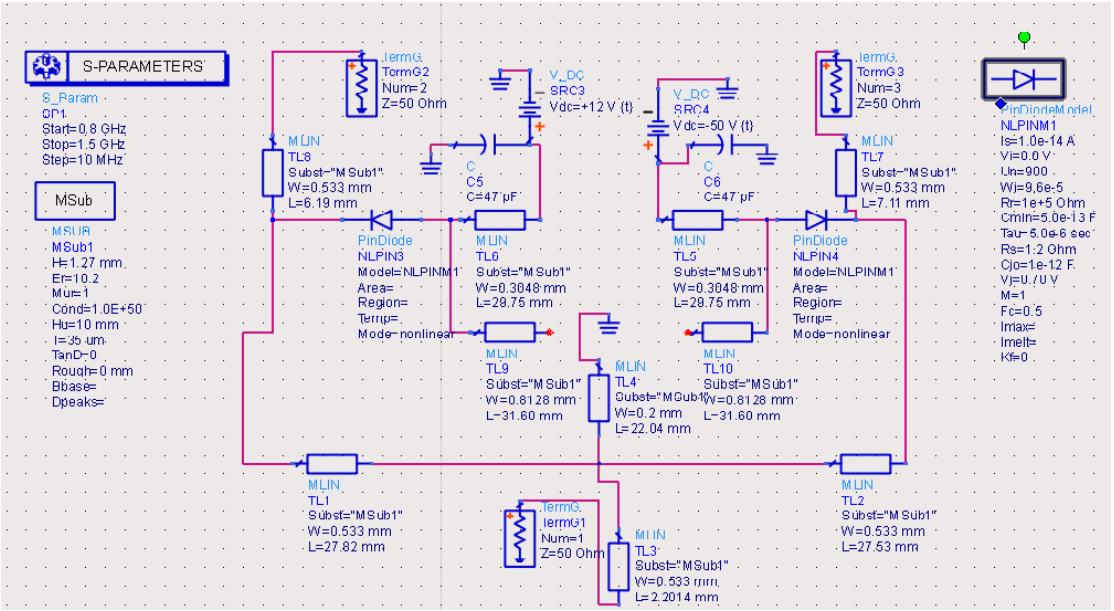

FIGURE 4.5: Mlines Schematics of SPDT switch

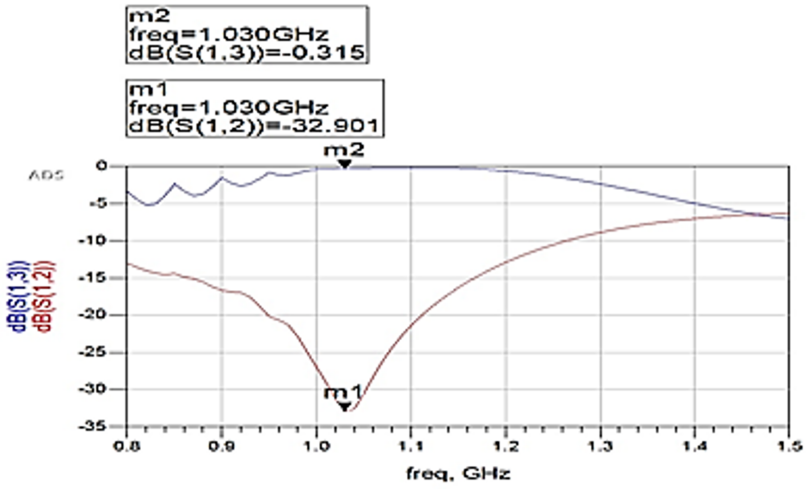

FIGURE 4.6: Insertion and Isolation Loss when transmission from antenna 1

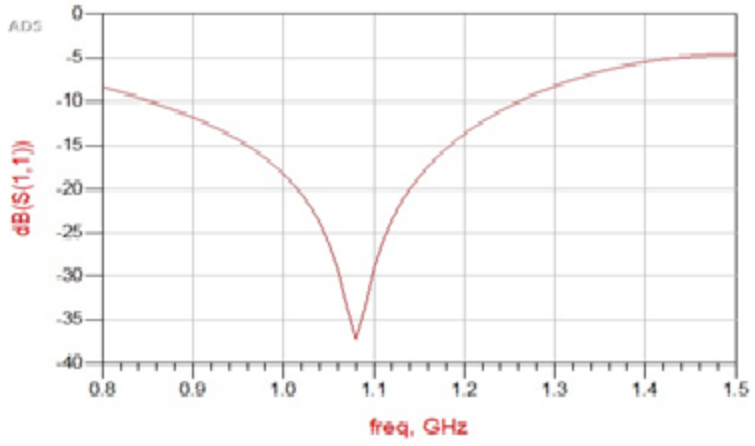

FIGURE 4.7: Return Loss when transmission from antenna 1

and insertion loss as shown in figure (4.6) and (4.7) are within the limits. The switch is providing a very good insertion loss of 0.315 dB and isolation of 32.90 dB from other port. Therefore the next step is to design the SPDT switch using the dimensions calculated.

4.6 Layout design and Simulations

The PCB layout is drawn in ADS2016 as shown in Figure (4.8) using the dimesnions already finalized during Mline simulations. The layout is designed in the Layout ADS module using the dimensions calcuated during the simulations. The overall dimensions of the SPDT switch layout came out as 25x25 mm.

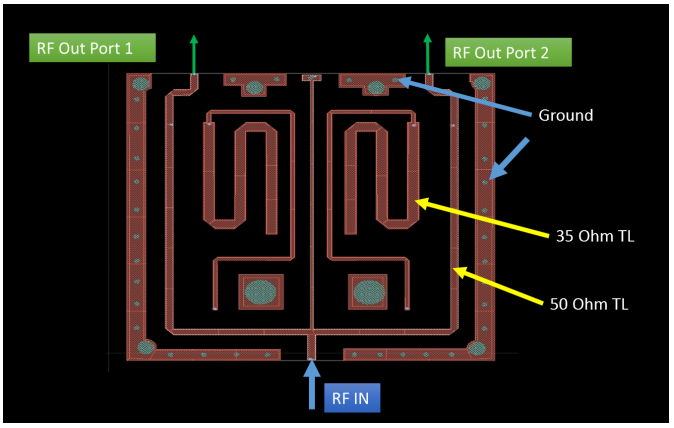

FIGURE 4.8: Layout of proposed design

4.6.1 Co-Simulation of Proposed Design & Results

In order to verify the veracity of physical layout, the same was simulated using the schematic ADS module in which the layout design was imported and design parameters were added in order to simulate the complete switch (Figure 4.9). The simulations were carried out keeping in consideration the two scenarios for transmission, i.e transmission from antenna 1 or antenna 2.

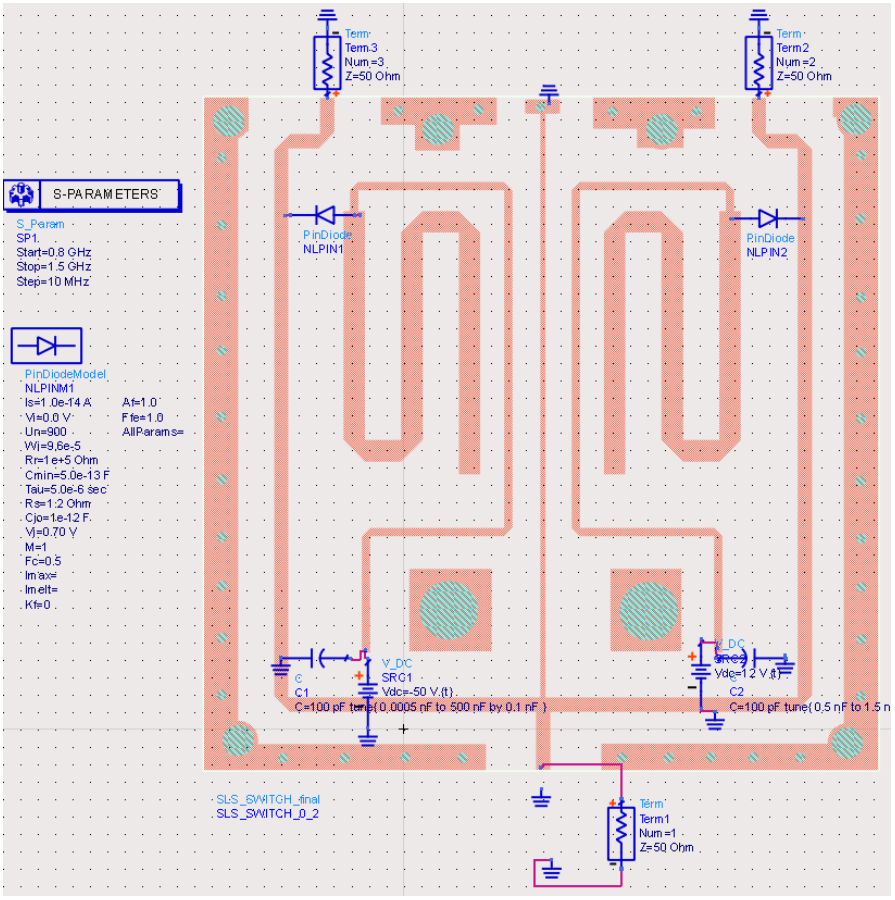

FIGURE 4.9: Schematic design of proposed SPDT Switch

4.6.2 Transmission from antenna 1

When upper antenna is selected for transmission, signal power at frequency 1030MHz travels from transmitting port to the upper antenna Port i.e. from port 1 to port 2. The signal flow is shown in Figure (4.10). Insertion Loss and Isolation while

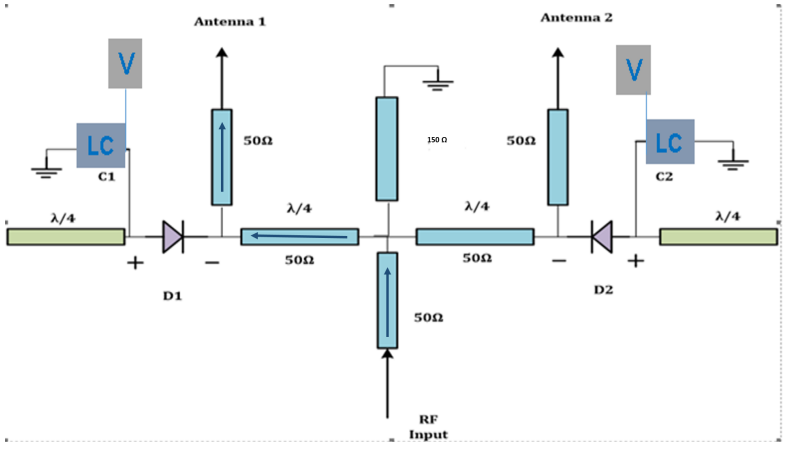

FIGURE 4.10: Transmission from Antenna 1

transmission from Antenna 1 is shown in Figure (4.11)

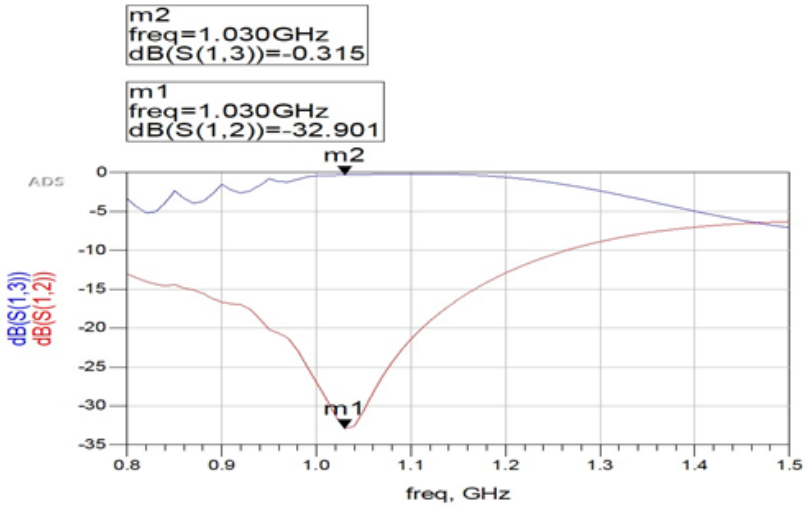

FIGURE 4.11: Insertion and Isolation Loss when transmission from antenna 1

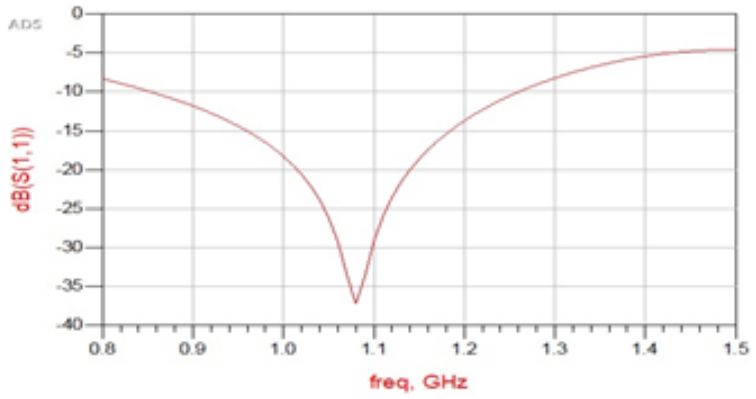

FIGURE 4.12: Return Loss when transmission from antenna 1

4.6.3 Transmission from Antenna 2

When lower Antenna is selected for transmission, signal power at frequency 1030MHz travels from transmitting port to the antenna Port 2 i.e. from port 1 to port 3. The signal flow is shown in Figure (4.13). Insertion Loss and Return Loss are shown in Figure (4.14) and Figure (4.15) respectively.

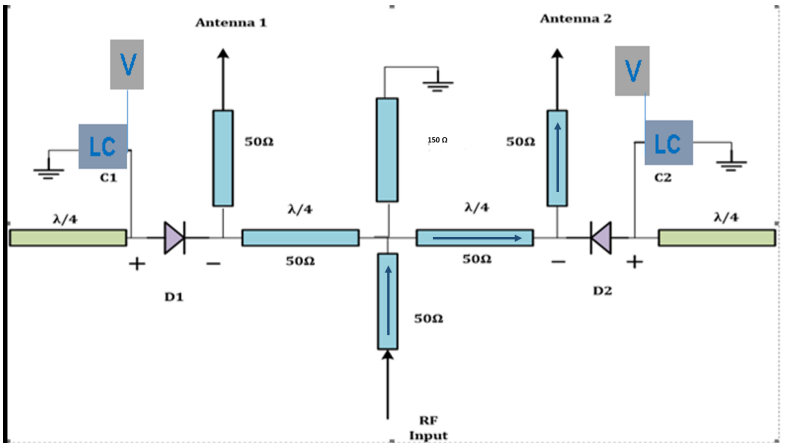

FIGURE 4.13: Signal Flow for Transmission from Antenna 2

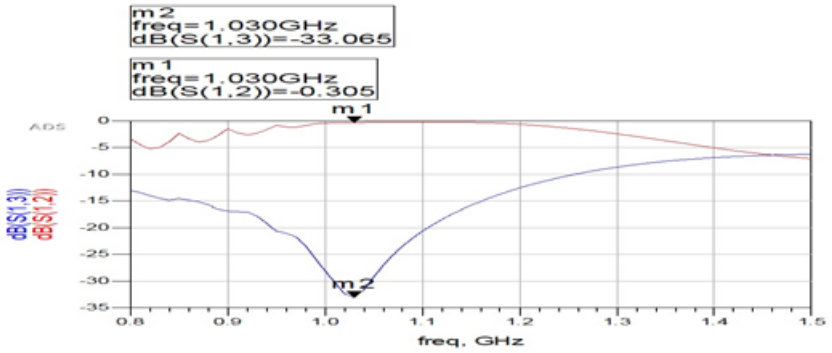

FIGURE 4.14: Isolation and Insertion Loss when transmission from Antenna 2

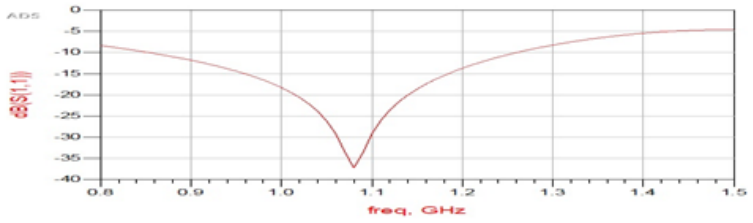

FIGURE 4.15: Return Loss when transmission from Antenna 2

4.7 Fabrication of Simulated Design

After successful designing and simulations of SPDT switch, the high power design is fabricated on the Rogers 6010.2LM sheet. The measured dimensions of RF SPDT minituarized switch are 25x25 mm are shown in figure 4.16. For ease of operation, RF connectors were installed at the input and output ports and power is provided for the operation of diodes using the electrical wires as shown in the picture.

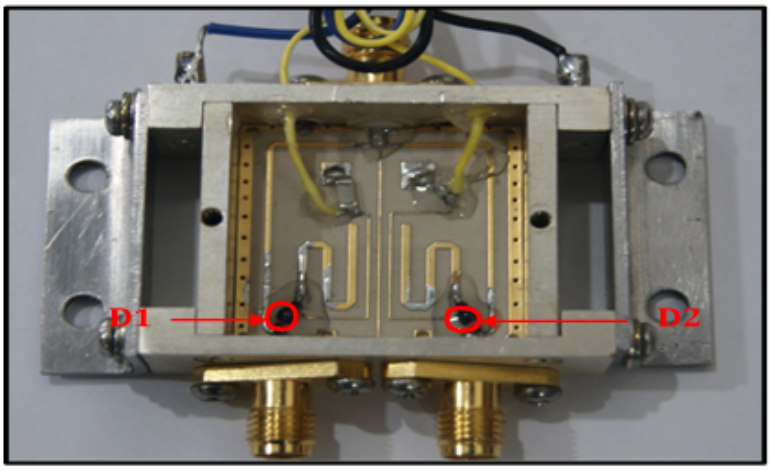

FIGURE 4.16: Fabricated prototype

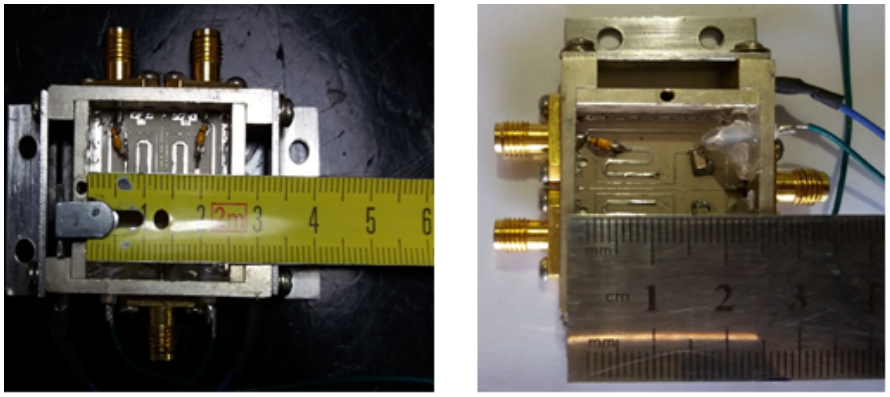

FIGURE 4.17: Dimensions of SPDT Switch 25x25 mm

4.8 Test environment and prototype measurements

For the DC biasing of PIN diodes two different potential levels, -50V and +12V are required which are provided by Power Flex CPX400D power supply. Rohde and Schwarz Vector Network Analyzer ZVL is used to measure the S-parameters. The connections of power supplies were tested by multi-meter. The positive and negative required potentials were set with respect to zero potential. After connecting power source, the module is tested using network analyzer to analyze the response over the range of frequencies and to measurement of scattering parameters. The two ports of network analyzer are first calibrated then the DUT is connected between the two ports, where port1 is the input port and port2 is

the output port. The test setup is show in Figure (4.18). Scattering parameters

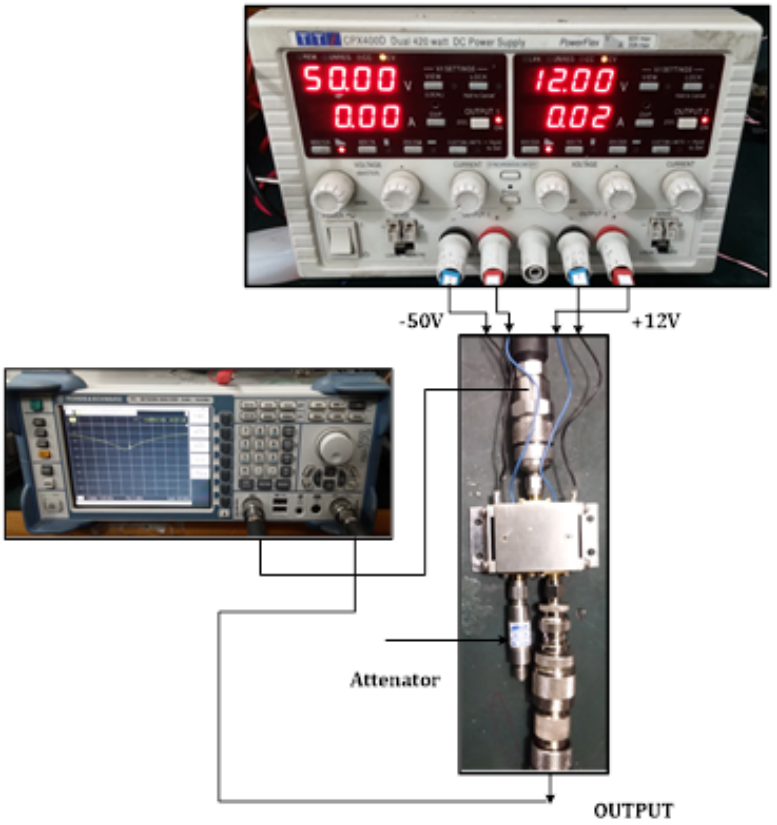

FIGURE 4.18: DUT test setup

are measured to estimate Insertion loss and isolation. The data collected from measurements and simulations is plotted on the graph in MATLAB.

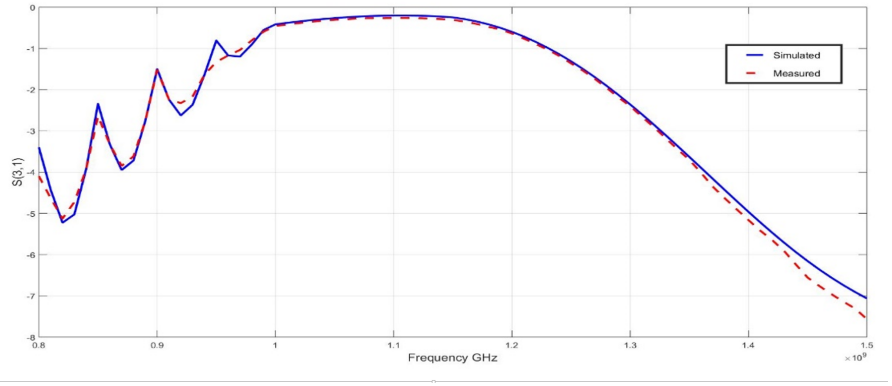

FIGURE 4.19: Comparison of Insertion Loss b/w measured & simulated results of SPDT Switch during transmission from antenna 1

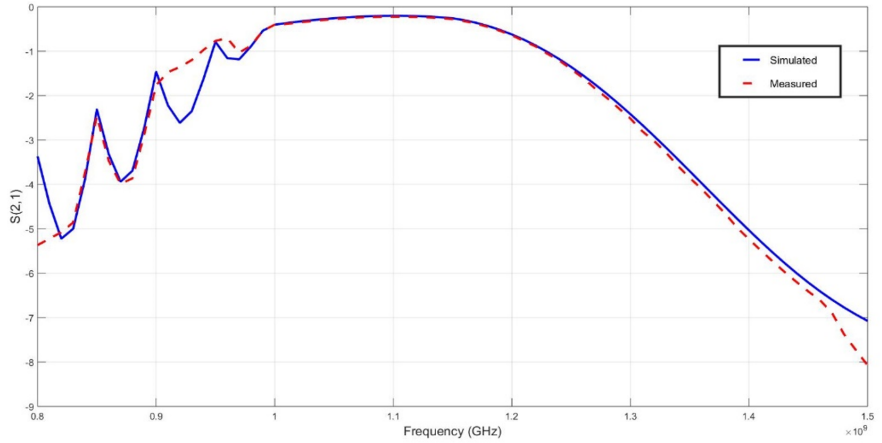

FIGURE 4.20: Comparison of Insertion Loss b/w measured & simulated results of SPDT Switch during transmission from antenna 2

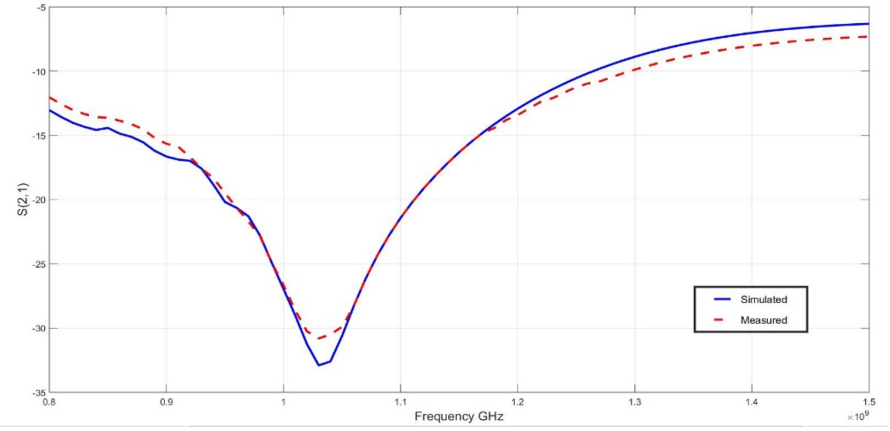

FIGURE 4.21: Comparison of Isolation b/w measured & simulated results of SPDT Switch during transmission from antenna 1

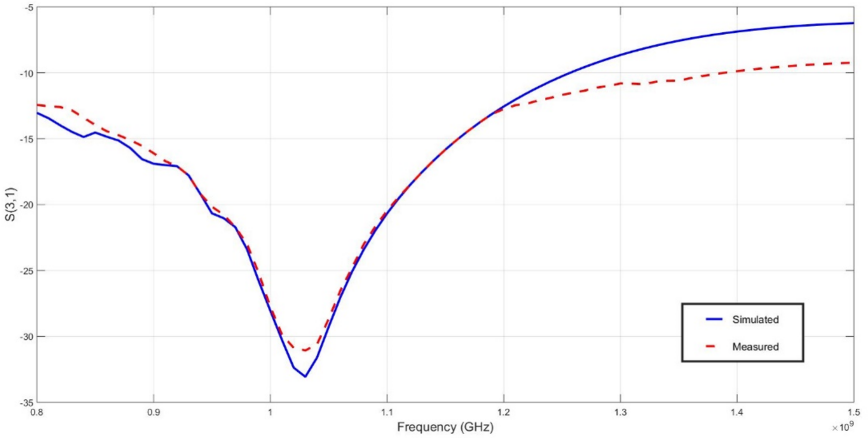

FIGURE 4.22: Comparison of Insertion Loss b/w measured & simulated results of SPDT Switch during transmission from antenna 1

4.9 Switching Time of SPDT Switch

The switching time of SPDT switch was measured using the agilent signal generator, oscilloscope and function generator. The RF input signal was generated through signal generator and a control signal was transmitted through function generator, resultantly, the response was measured on the oscilloscope. The results thus acheived shows the switch ON time of 50 ns, while the rise time 40 ns.

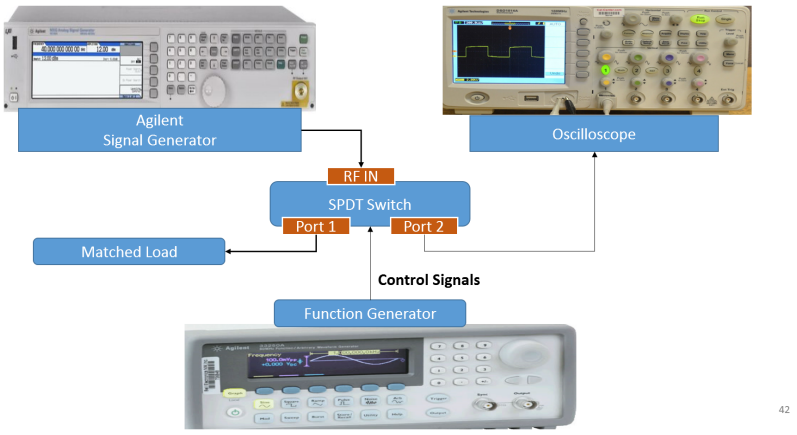

FIGURE 4.23: Setup for Switching Time Measurement

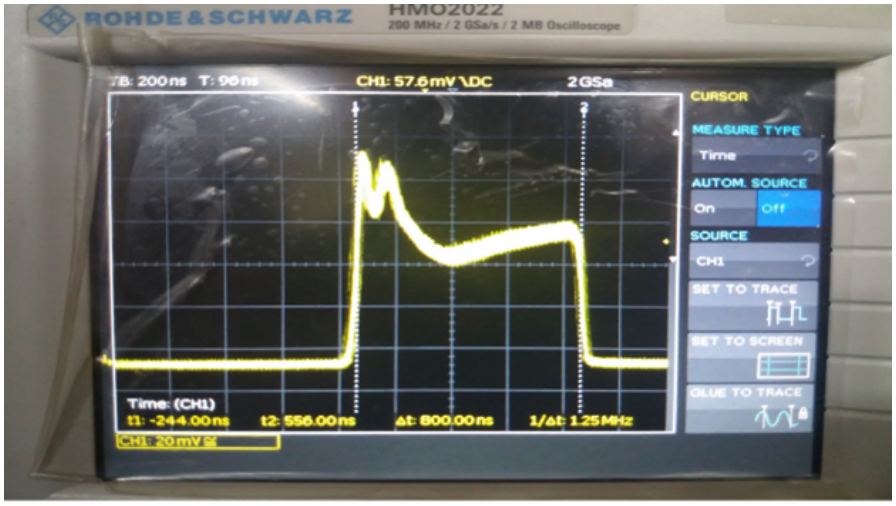

FIGURE 4.24: Complete Pulse duration of 800 ns on oscilloscope

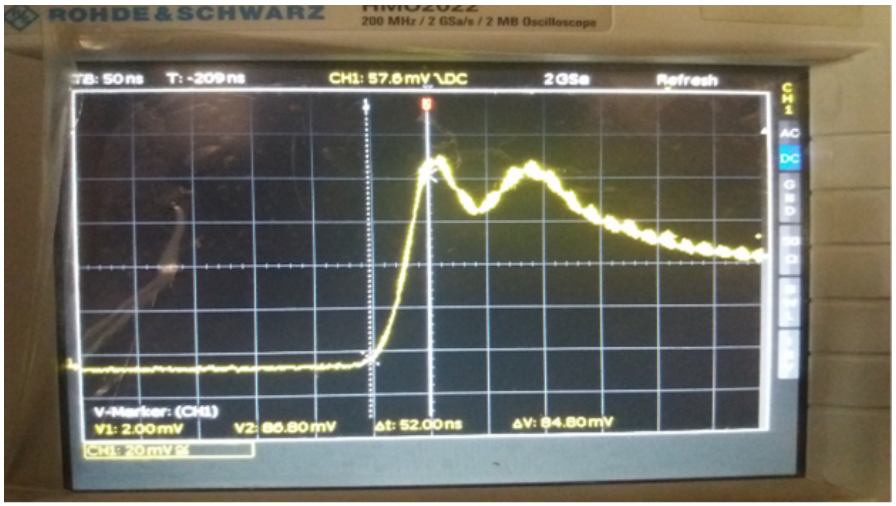

FIGURE 4.25: Switching On time results on oscilloscope

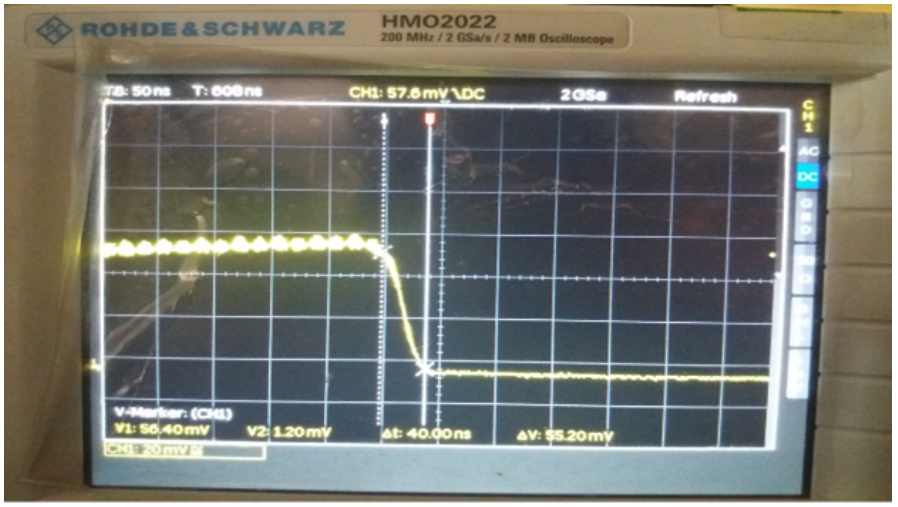

FIGURE 4.26: Switching OFF time results on oscilloscope

4.10 Discussion

After taken measurements, measured and simulated results are compared in Table 4.6. From comparison, it can be observed that isolation of more than 30dB was achieved in simulations with insertion loss of less than 1dB. In measured results it has been found that there is a slightly change in the results but still results are very closed to the desired one i.e. Isolation is very close to 30dB measured on antenna 1 & antenna 2 insertion loss of less than1 dB .

	Simulated Results	Measured Results
Isolation measured on Antenna 1	-32.15 dB	-31.2dB
Isolation measured on Antenna 2	-32.15 dB	-31.2dB
Insertion loss when transmission from Antenna 1	-0.315 dB	-0.32 dB
Insertion loss when transmission from Antenna 2	-0.315 dB	-0.32 dB

TABLE 4.6: Comparison between simulation and measured results

Chapter 5

CONCLUSIONS AND FUTURE WORK

5.1 Conclusion

A high power miniaturized high power SPDT switch using a combination of PIN diodes has been successfully designed, simulated, fabricated and tested. A detailed understanding of techniques used for development of SPDT switches were discussed in detail along with the properties of PIN diodes in comparison with other switching techniques. The power handling capability for substrate materials including FR4 and Rogers 6010.2 LM has been calculated and compared. It was observed that FR4 material has high attenuation coefficient due to conductor and dielectric loss as compared with Rogers 6010.2 LM. Moreover a comparison of the substrates was also done using the Line Cal tool of ADS for selection of substrate found suitable for miniaturization of design. The design methodology is implemented using ideal transmission lines by using the state of the art ADS2016 software for proof of concept. The design was further simulated by considering the properties of Rogers RT/Duroid 6010.2LM and selected PIN diode. The results shows that the isolation of -32.5 dB is achieved with an insertion loss of just -0.31 dB. The design was translated into a PCB hardware using the Roger R/T

Duroid 6010.2LM sheet and the module was testing using Aglient Vector Network Analyzer (VNA). Measured results showed that isolation of around -31.2 dB and insertion loss of approximately -0.32dB was achieved successfully.

The work provides understanding of linking the theoretical knowledge with the practical scenario and clear understanding of simulated vis a vis measured results were achieved. Miniaturized RF PCB layout with power handling capability of 60 dBm in a small design are the bench marks that are achieved. Moreover, method for calculation and comparison of power handling capability of different microstrip lines was also presented.

5.2 Future work

In the era of modern technologies where latest developments are focused towards miniaturization, the availability of high power RF technique would open doors for radar developments on drones and small UAVs. Since transmission, elements are the most vital elements for radar design, their development and testing for utilization on latest developments will continue in future. The design can further be modified and evaluated for a vast frequency range. The insertion loss and isolation can be further improved by removal of shortcomings of this work.

Bibliography

[1] R. W. Keyes, "Miniaturization of electronics and its limits", in *IBM Journal of Research and Development,* vol. 44, no. 1.2, pp. 84-88, Jan. 2000.

[2] D. V. Brovchenko, "Application features of UAVs different types", *2015 IEEE International Conference Actual Problems of Unmanned Aerial Vehicles Developments (APUAVD),* Kiev, 2015, pp. 26-29.

[3] A. Al-Kaff, F. M. Moreno, A. de la Escalera and J. M. Armingol, "Intelligent vehicle for search, rescue and transportation purposes", *IEEE International Symposium on Safety, Security and Rescue Robotics (SSRR),* Shanghai, 2017, pp. 110-115.

[4] M. Weib, O. Peters and J. Ender, "three dimensional SAR system on an UAV", *IEEE International Geoscience and Remote Sensing Symposium, Barcelona,* 2007, pp. 5315-5318

[5] "International Civil Aviation Organization Asia And Pacific Guidance Material on Comparison of Surveillance Technologies Edition 1.0 September 2007",*www.icao.int* [Online] Available : https://www.icao.int/APAC/Documents/edocs/cns/gmsttechnology.pdf [Accessed: 15 March 2017]

[6] S. Neemat and M. Inggs, "Design and implementation of a digital real time target emulator for secondary surveillance radar / identification friend or foe", in *IEEE Aerospace and Electronic Systems Magazine*, vol. 27, no. 6, pp. 17-24, June 2012.

[7] ICAO *International Standards And Recommended Practices* Annex 10, Volume 4, Amendment 89 pp 285-320 (2014)

[8] G. Slovin, M. Xu, R. Singh, T. E. Schlesinger, J. Paramesh and J. A. Bain, "Design Criteria in Sizing Phase-Change RF Switches", in *IEEE Transactions on Microwave Theory and Techniques,* vol. 65, no. 11, pp. 4531-4540, Nov. 2017.

[9] "Categories of RF Switches" *qsl.net* [Online]. Available : https:/www.qsl.net/va3iul/RFSwitches/RFSwitches.pdf. [Accessed: 15 April 2017]

[10] W. E. Doherty, Jr., R. D. Joosi, *THE PIN DIODE CIRCUIT DESIGNERS HANDBOOK* , California : Microsemi Corporation (1998)

[11] Jean-Jacques DeLisle, *6 Degrees of Microwave and RF/Microwave Switch Separation* [Online]. Available : www.mwrf.com/passive-components/6-degrees-microwave-and-rfmicrowave-switch-separation [Accessed: 15 Mayl 2017]

[12] W. Jablonski, "A new method of the design and technology of PIN diodes", *12th International Conference on Microwaves and Radar. MIKON-98. Conference Proceedings,* Krakow, 1998, pp. 69-73 vol.1

[13] Y. M. Madany, N. E. H. Ismail and H. A. Hassan, "Analysis and design of wideband single-pole double-throw (SPDT) transmitter/receiver (T/R) switch with PIN diode for transceiver systems", *2013 IEEE Antennas and Propagation Society International Symposium (APSURSI),* Orlando, FL, 2013, pp. 1004-1005.

[14] C.A.Balanis,*Antenna Theory Analysis and Design*, New York : John Wiley & Sons, (2005)

[15] "Microwave Theory", *madmadscientist.com* 2017. [Online]. Available:http://www.madmadscientist.com/html/Theory.htm. [Accessed: 19-June- 2017].

[16] N. A. Shairi, B. H. Ahmad and A. C. Z. Khang, "Design and analysis of broadband high isolation of discrete packaged PIN diode SPDT switch for wireless data communication", *IEEE International RF & Microwave Conference,* Negeri Sembilan, 2011, pp. 91-94

[17] M. U. Nazir, M. Kashif, N. Ahsan and Z. Y. Malik, "PIN diode modelling for simulation and development of high power limiter, digitally controlled phase shifter and high isolation SPDT switch", *Proceedings of 2013 10th International Bhurban Conference on Applied Sciences & Technology (IBCAST), Islamabad,* 2013, pp. 439-445.

[18] N. A. Shairi, A.M. Zobilah, B.H. Ahmad and Z. Zakaria, "Design Comparison of RF SPDT Switch with Switchable Resonators for WiMAX and LTE in 3.5 GHz Band", *International Journal of Applied Engineering Research* ISSN 0973-4562 Volume 12, Number 20 (2017) pp. 9614-9618.

[19] A. Yaman, A. Oncu and E. Gose, "The design and analysis of PIN diode SPDT Switch and feeding circuit for Security Purpose Pulse Doppler Radar", *6th International Conference on Recent Advances in Space Technologies (RAST)*, Istanbul, 2013, pp. 207-211

[20] Bahl, I.J., Gupta K. C., *Average Power Handling Capability of Microstrip Lines*, IEE proceedings on H Microwaves, Optics and Antennas, vol.127, no.1, p.40,1980.

[21] J. Bahl and D. K. Trivedi, *A Designer's Guide to Microstrip Line, Microwaves*, New York : Wilsons 1977, pp. 174-182

[22] "Rogers Cooperation RT/duroid 6006/6010 data sheet", *Rogerscorp.com* [Online]. Available :https://www.rogerscorp.com/.../36/RT-duroid-6006-6010-Laminates.aspx [Accessed: 15-July-2017]

[23] "PCB Trace Width", *eeweb.com* [Online]. Available :https://www.eeweb.com/tools/external-pcb-trace-width [Accessed: 15-December-2017]

[24] "High Power PIN Diode Data Sheet" *cdn.macom.com* [Online]. Available :httpshttps://cdn.macom.com/datasheets/MA4P-MELF-HIPAX-Series.pdf [Accessed: 15-December-2017]

[25] "Principles of measuring high frequency networks with network analyzer by Keysight Technologies" *keysight.com* [Online] Available : https//www.keysight.com/en/pcx-x2015001 [Accessed: 15 August 2017]

[26] "Technical manual of E5071C ENA Vector Network Analyzer by Keysight Technologies" *keysight.com* [Online] Available : https/l/iterature.cdn.keysight.com/litweb/pdf/5989-5478EN.pdf [Accessed: 15 August 2017]

[27] "Getting Started Guide: Agilent E4440A Spectrum Analyzer" *keysight.com* [Online] Available : https//literature.cdn.keysight.com/litweb/pdf/E4440-90607.pdf [Accessed: 30 August 2017]